American Mineralogist, Volume 73, pages 20–47, 1988

Devonian and Carboniferous metamorphism in west-central Maine: The muscovite-almandine geobarometer and the staurolite problem revisited

M. J. Holdaway
Department of Geological Sciences, Southern Methodist University, Dallas, Texas 75275, U.S.A.
B. L. Dutrow
Department of Geology, Louisiana State University, Baton Rouge, Louisiana 70803, U.S.A.
R. W. Hinton*
The Enrico Fermi Institute, The University of Chicago, Chicago, Illinois 60637, U.S.A.

Abstract

Important thermal metamorphic events in west-central Maine occurred at 400 Ma (M_2), 394–379 Ma (M_3), and 325 Ma (M_5). Each is closely associated with emplacement of S-type granites, such that the isograd patterns produced in the surrounding pelitic schists generally follow plutonic outlines. From north to south, grade of metamorphism varies from chlorite to sillimanite–K-feldspar–muscovite.

Mineral-chemistry studies on M_3 and M_5 indicate the following: (1) Much staurolite-grade chlorite is retrograde as demonstrated by the lack of a consistent relation between biotite composition and presence or absence of chlorite, given the restricted range of X_{H_2O} allowed in these reduced graphitic rocks. Consequently, the first sillimanite-forming reaction for many pelitic schists in Maine does not involve chlorite. (2) Garnet zoning patterns are prograde in rocks of the staurolite zone and retrograde in rocks of higher grade. (3) Presence of graphite and nearly pure ilmenite suggests low Fe^{3+} in micas and allows for end-member calculations that include a "Ti biotite" ($KTi\square(Fe,Mg)AlSi_3O_{10}(OH)_2$) and a "Ti muscovite" ($KTi(Fe,Mg)AlSi_3O_{10}(OH)_2$). (4) Staurolite contains about 3 H (48-oxygen basis) and shows subtle indications of nonideality in Fe-Mg K_D relationships.

Garnet-biotite geothermometry indicates the following average temperatures for the first occurrence of minerals: staurolite—510 °C, sillimanite—580 °C, sillimanite–K-feldspar—660 °C. The muscovite-almandine-biotite-sillimanite (MABS) geobarometer is calibrated on the basis of an average M_3 pressure of 3.1 ± 0.25 kbar such that staurolite + muscovite break down directly to sillimanite + almandine + biotite immediately above the sillimanite-andalusite phase boundary. On the basis of this geobarometer, the M_5 rocks inside the second sillimanite isograd crystallized at 3.8 kbar.

The muscovite-quartz dehydration boundary shows excellent agreement with garnet-biotite temperatures and MABS pressure for the second sillimanite isograd in M_5 if reasonable models for behavior of fluids in reduced graphitic pelites are assumed. The staurolite-quartz dehydration boundary predicts temperatures about 60 °C above the garnet-biotite temperatures for the first sillimanite isograd in M_3. However, this discrepancy can be partially eliminated by assuming a regular pseudobinary staurolite solution model with W_G = 15 kJ per tetrahedral Fe site. Nonideality in staurolite solid solution may also explain staurolite K_D relationships that involve reversals in K_D values.

The progressive southward increase in pressure from early M_2 (2.35 kbar) to M_3 (3.1 kbar) to M_5 (3.8 kbar) over a 75-m.y. period requires a net increase of about 5 km of rock during a time when much of New England was suffering erosion. This P increase is believed to have been the combination of two effects: (1) as the locus of metamorphic heat moved southward, the depth of metamorphism increased by 2 to 3 km over a distance of 125 km laterally, implying postmetamorphic tilting of the area and/or differences in original topography; and (2) at any given place, P increased with time because of development of a widespread Devonian volcanic highland and correlative emplacement of granites at shallow levels.

The extensive terrane of M_5, which varies from K-feldspar–bearing to K-feldspar–absent rocks, marks incipient granite melting immediately below the present rocks at 3.8 kbar, 660 °C; local T variations probably reflect local differences in degree of mobilization of magma and fluids. This presumably occurred above the gently north-dipping contact of the Sebago batholith exposed south of the M_5 rocks.

* Present address: Grant Institute of Geology, Edinburgh, Scotland EH93JW.

0003–004X/88/0102–0020$02.00

Introduction

West-central Maine provides a unique opportunity to unravel the complexity of Acadian and Hercynian metamorphic events, as it lies in the transitional zone between slightly metamorphosed rocks to the north and high-grade metamorphism to the south. Within this zone, the distinctive overprints of three thermal metamorphic events have been preserved. Previously, the metamorphic petrology, isograds, mineral reactions, and metamorphic history of this region, bounded by the cities of Augusta, Lewiston, Norway, Rangeley, Kingfield, and Madison (Fig. 1), have been summarized by Holdaway et al. (1982) and Guidotti et al. (1983). This area is one of dominantly pelitic metamorphic rocks and S-type granites, mainly of the New Hampshire Magma Series, and it represents the transition from chlorite-zone rocks to the prevailing upper amphibolite–grade metamorphism that is dominant in southern Maine, southern New Hampshire, and central Massachusetts. Lithologic units and their ages are summarized by Holdaway et al. (1982) and references therein.

The present report provides data on mineral chemistry and metamorphic conditions for the dominant M_3 and M_5 metamorphism of the region covered by Holdaway et al. (1982). Pressure estimates for M_3 are deduced from biotite-garnet geothermometry combined with aluminum silicate stability relations. In addition, the potential for a muscovite-almandine-biotite-sillimanite (MABS) geobarometer is examined and applied to estimate the pressure of M_5. Garnet-biotite geothermometry, combined with experimental stability data on muscovite-quartz and staurolite-quartz, allows for a test of models for the behavior of C-H-O fluids in pelitic rocks. These data are then integrated with the present understanding of the metamorphic history of Maine to provide insight into the conditions and causes of metamorphism in Maine.

These metamorphic rocks are ideal for evaluating and formulating pelitic geothermometers and geobarometers because the lack of synchronous deformation allows for the assumption of nearly constant pressure during each thermal event, and ubiquitous presence of graphite allows for the assumptions of low f_{O_2} and low and/or approximately constant Fe^{3+} content in Fe-bearing phases.

Brief summary of metamorphic events

Holdaway et al. (1982) summarized the sequence of metamorphic events of the region considered here. A brief summary of these events, as they are now interpreted, follows.

M_1

The first event, slightly older than 400 Ma, produced widespread chlorite-zone metamorphism synchronous with S_2 schistosity (Guidotti, 1970). Much of the area between Madison, Farmington, and Kingfield (Fig. 1) has suffered only this event, and temperature has not been significantly higher in this area during the subsequent events.

M_2

Following M_1, a widespread thermal event produced staurolite, staurolite-andalusite, and andalusite in rocks of appropriate composition and grade (terms as in Guidotti, 1970). This event is easily recognized in much of the area between Farmington, Kingfield, and Rangeley (Fig. 1, Holdaway et al., 1982) where retrograde metamorphism has downgraded staurolite- and andalusite-bearing assemblages and in the process produced distinctive pseudomorphs. These authors estimated the timing of this event as $\geq 394 \pm 8$ Ma. Recently, Gaudette and Boone (1985) have obtained a whole-rock Rb-Sr age of 400 Ma on the Lexington batholith (Fig. 1). Dickerson and Holdaway (ms.) have correlated intrusion of this pluton with M_2. M_2 andalusite occurs as a relict mineral in several areas most recently affected by M_3 (Holdaway et al., 1982). A regional study of M_2 will be the topic of a future communication.

M_3

The most prevalent metamorphism in the area is regional-contact metamorphism spatially associated with the Mooselookmeguntic, Songo, Phillips, Livermore Falls, and Hallowell batholiths or groups of plutons (Fig. 1). Whole-rock Rb-Sr ages range from 394 to 379 Ma (Dallmeyer and Vanbreeman, 1978; Moench and Zartman, 1976). This metamorphism produced the grade sequence biotite → almandine → staurolite → sillimanite, all present with muscovite. Isograds broadly follow plutonic outcrops. No major retrogressive effects have been noted. Grade designations and their mineral assemblages (abbreviations after Kretz, 1983) for M_3 and M_5 are defined by number as follows:

1	Chl (M_3)
2	Bt + Chl (M_3)
3	Grt + Bt + Chl (M_3)
4	St + Grt + Bt (± Chl) (M_3)
5	Sil + St + Grt + Bt (M_3)
6	Sil + Grt + Bt (M_3)
6.5	Sil + Grt + Bt (within grade 7) (M_5)
7	Kfs + Sil + Grt + Bt (M_5)
8	Kfs + Sil + Grt + Bt (trace Ms) (M_5)

All assemblages contain Ms + Qtz + Gr ± Pl ± Tur. Complete distribution of mineral assemblages is shown in Figure 1 of Holdaway et al. (1982). Figure 1 (this report) displays M_3 isograds for the staurolite zone (grade 4), sillimanite zone (grades 5 and 6), and K-feldspar–sillimanite zone (grades 6.5 and 7 in M_5). Apart from the local appearance of M_2 andalusite, textures and compositions indicate that in grades 4 to 8, all prograde minerals equilibrated with M_3 or M_5 conditions.

M_4

The recent dating of the Lexington batholith at 400 Ma (Gaudette and Boone, 1985) puts the significance of M_4 for this area in doubt. The Hartland pluton, 15 km north-

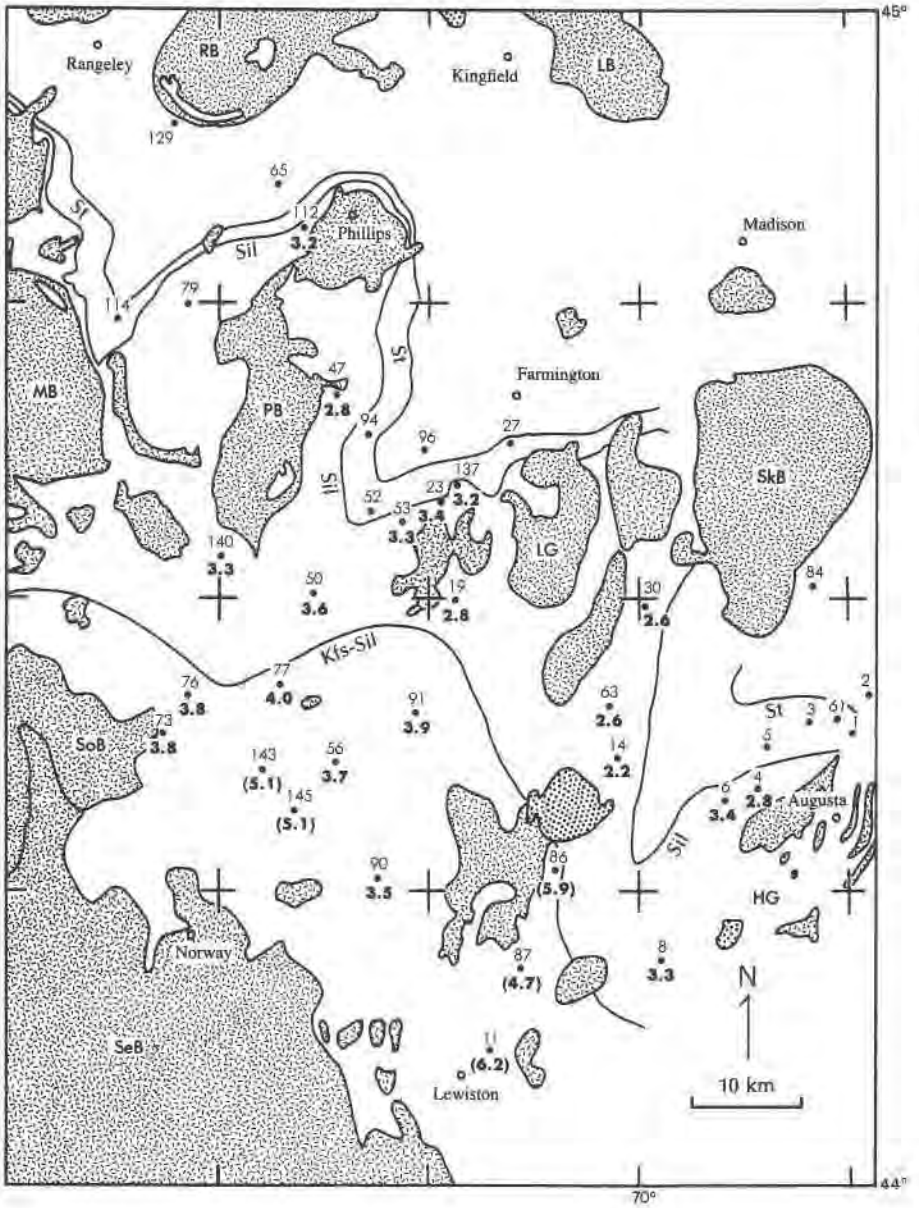

1	2	3	4
5	6	7	8
9	10	11	12
13	14	15	16

1. Rangeley
2. Phillips
3. Kingfield
4. Anson
5. Rumford
6. Dixfield
7. Farmington
8. Norridgewock
9. Bryant Pond
10. Buckfield
11. Livermore
12. Augusta
13. Norway
14. Poland
15. Lewiston
16. Gardiner

Fig. 1. Isograd map for M_3 and M_5 in west-central Maine. Isograds shown are M_3 staurolite (St), M_3 sillimanite (Sil), and M_5 K-feldspar–sillimanite (Kfs-Sil). Whole numbers refer to analyzed specimens. Bold decimal numbers indicate *P* determinations from Table 10 in kbar. Pressures in parentheses are those from grade 7 (Table 10) that may represent disequilibrium as discussed in text. Acidic plutonic units—pattern: MB = Mooselookmeguntic batholith, PB = Phillips batholith, LG = Livermore Falls group, HG = Hallowell group, RB = Reddington batholith, LB = Lexington batholith, SkB = Skowhegan batholith, SoB = Songo batholith, SeB = Sebago batholith (Hercynian). Gabbroic plutonic units—stipple. For names of quadrangles, see diagram and list at right. For complete distribution of mineral assemblages, see Holdaway et al. (1982). Modified from Holdaway et al. (1982), Henry (1974), Dutrow (1985), and Evans and Guidotti (1966). Igneous contacts from Osberg et al. (1985). M_2 metamorphism is not shown and will be discussed in a future contribution (see also Dickerson and Holdaway, ms.; Holdaway et al., 1986a). Isograds stop near Skowhegan batholith because its metamorphism involves andalusite and may be M_2.

east of the Skowhegan pluton (Fig. 1) is the closest dated pluton (whole-rock Rb-Sr, Dallmeyer et al., 1982) at 362 Ma, the age Holdaway et al. (1982) assumed for M_4. We tentatively conclude that M_4 did not affect the area under study.

M_5

Recent isotopic studies for the Sebago batholith (Fig. 1) give Hercynian ages of 325 Ma (Hayward and Gaudette, 1984) and 324 ± 3 Ma (Aleinikoff et al., 1985)

using Rb-Sr whole rock and U-Pb on zircon, respectively. Lux and Guidotti (1985) and Guidotti et al. (1986) have pointed out that much of the higher-grade area to the south of the M_3 plutons has probably equilibrated to the thermal events associated with the emplacement of this younger Sebago batholith, thereby preserving only post-M_3 effects. The sillimanite–K-feldspar isograd (Fig. 1) shows a general spatial relation to the Sebago contact. Much of this area is highly migmatitic and pegmatitic, and the age of these igneous rocks may well correlate with that of the Sebago batholith. Lux and Guidotti (1985) and Guidotti et al. (1986) have suggested that the effects of the Sebago event may extend as far as 30 km to the north and certainly are responsible for the sillimanite–K feldspar isograd. One possible shortcoming of this interpretation is the absence of an obvious "hinge" effect (Guidotti, 1970), a retrograded zone of M_3 rocks where lower temperatures from the Sebago event might have downgraded the rocks far north of the pluton. However, Guidotti et al. (1986) have noted some downgrading in the Rumford quadrangle. We designate this Hercynian higher-P, higher-T event M_5 and suggest that those rocks south of the second sillimanite isograd (grades 6.5 and 7) suffered its effects. It should be pointed out that M_3 and M_5 were originally mapped as a single metamorphic sequence (e.g., Holdaway et al., 1982). The principal reasons for separating M_3 and M_5 are the age differences between plutons, the spatial association with the plutons, and important differences in T and P as discussed below.

The rocks under consideration for this report have suffered M_3 and/or M_5 depending on their grade and map location. M_2 is discussed in more detail by Holdaway et al. (1986a) for a four-quadrangle area in the Kingfield region, by Dickerson and Holdaway (ms.) for the Bingham area, north of the Kingfield and Anson quadrangles, and by Dutrow and Holdaway (in prep.) for the Farmington area.

Analytical methods

For the area of M_3 and M_5 in Figure 1, 40 polished sections of low-variance rocks were prepared for microprobe work. Locations are shown by numbers in Figure 1. Microprobe analyses were done on an automated JEOL-733 microprobe at SMU with KRISEL automation that uses the correction procedure of Bence and Albee (1968) modified by Albee and Ray (1970). Beam current was 20 nA, accelerating potential was 15 kV, and beam diameter was focused to ~2 μm for staurolite, garnet, and ilmenite and to 10 μm for phyllosilicates and plagioclase. Standards included a number of analyzed silicates and oxides. For each mineral, five or six analyses were taken from one portion of the thin section as near as possible to the garnet being analyzed. Analyses were for 30 s or 60 000 counts. For staurolite, all major elements were renormalized to standards to minimize drift, and Al and Fe values were multiplied by constants to bring the analyses into agreement with previous good-quality microprobe and wet-chemical analyses, a procedure described by Holdaway et al. (1986b). Ilmenite (Fe, Ti, Mn) and plagioclase (Na, Ca) analyses were also renormalized to standards to minimize drift. For garnet, a regularly spaced traverse across one or two grains was used. The core and intermediate-zone analyses were grouped and averaged on the basis of chemical similarity. Garnet-biotite geothermometry indicated that all garnet rim analyses (~5 μm from rim) showed retrograde temperatures, and these values are not given here. Biotite analyses were taken from several grains within 30 to 100 μm of the garnet being analyzed. Each biotite was analyzed immediately before or after the coexisting garnet using the same analysis file.

Presence of graphite and/or nearly pure ilmenite ($\leq$4% hematite solid solution) in every rock indicates that Fe^{3+} should be minor and approximately constant in most of the minerals. Consistent with the assumption of low Fe^{3+}, mineral stoichiometries were determined by normalizing to the indicated number of ions: micas—22 oxygens, chlorite—28 oxygens, feldspars—8 oxygens, garnet—8 cations, and ilmenite—2 cations. For staurolite, stoichiometry was determined by normalizing (Si + Al) to 25.53 as discussed below.

Ion-microprobe analyses were done on two ilmenite specimens (see Table 8) using an AEI IM-20 ion microprobe at the University of Chicago. The instrumental configuration was described by Steele et al. (1981), and the analytical configurations were similar to those described by Jones and Smith (1984). The ion yields were based on Corning borosilicate glasses, except Li (staurolite), Na (plagioclase), Sc (hibonite), and Nb (assumed to be the same as Zr). Analyses were made by scanning from mass 100 to mass 7, counting for 1 s at each mass. Elements not listed in Table 8 were not detected. These semiquantitative analyses will be affected by matrix-dependent factors and are estimated to be between 0.5 and 2 times the correct values.

In order to save space but provide the maximum amount of data, the major-element analyses are presented in Appendix Table 1 as stoichiometric analyses only, plus the oxide total. Analyses are listed in order of increasing grade designation (see above). Within each grade, analyses are given in order of increasing temperature using a slightly modified Ganguly-Saxena (1984) biotite-garnet geothermometer (discussed in the section on geothermometry). In the text, tables are provided to illustrate the average compositions of minerals with increasing grade.

Mineral chemistry and petrologic interpretation

Petrologic interpretation of the present study area is provided in a paper by Holdaway et al. (1982). This section adds aspects to their interpretation that have become possible as a result of detailed mineral chemistry.

To a very good approximation, the metamorphic rocks studied within a given metamorphic event (M_3 or M_5) may be regarded as a simple sequence of mineral assemblages that have similar bulk compositions, f_{O_2} controlled at a reducing value, X_{H_2O} controlled over a narrow range, and T (metamorphic grade) as the principal intensive variable. The thin sections chosen for study were selected on the basis of minimum variance, and each grade designation (given above) represents a *single* assemblage. Thus, changes in mineral assemblages and zoning are mainly a response to changes in T. In support of this simplified view are (1) the thermal (limited time) nature of the metamorphism, (2) the prevalence of graphite and nearly pure ilmenite, and (3) the fact that, with a few noted exceptions, the approach works. The section on

TABLE 1. Summary of average muscovite stoichiometry by grade, based on 22 oxygens

Grade:	3	4	5	6	6.5	7	8
Si	6.07(3)	6.05(3)	6.04(3)	6.04(2)	6.05(2)	6.07(1)	6.04
^{iv}Al	1.93(3)	1.95(3)	1.96(3)	1.96(2)	1.95(2)	1.97(1)	1.96
^{vi}Al	3.78(8)	3.82(4)	3.80(1)	3.76(4)	3.74(2)	3.71(2)	3.69
Ti	0.03(1)	0.03(1)	0.05(1)	0.06(1)	0.08(1)	0.08(2)	0.11
Fe	0.13(4)	0.10(1)	0.10(1)	0.11(2)	0.12(1)	0.13(1)	0.12
Mg	0.13(8)	0.09(2)	0.10(1)	0.11(2)	0.11(1)	0.12(1)	0.13
Σ(vi)	4.07(4)	4.04(1)	4.04(1)	4.04(1)	4.05(1)	4.04(1)	4.05
K	1.61(2)	1.56(9)	1.59(5)	1.67(8)	1.71(5)	1.83(3)	1.85
Na	0.29(6)	0.35(9)	0.34(6)	0.26(7)	0.21(5)	0.12(2)	0.09
Ba	0.01(0)	0.01(1)	0.01(0)	0.01(0)	0.01(1)	0.01(0)	0.01
Σ(xii)	1.91(3)	1.93(2)	1.95(2)	1.95(2)	1.93(3)	1.95(1)	1.95
Ba-ms	0.005	0.005	0.005	0.005	0.005	0.005	0.005
Ti-ms	0.015	0.015	0.025	0.030	0.040	0.040	0.055
phl-ann	0.035	0.020	0.020	0.020	0.025	0.020	0.025
ce	0.010	0.020	0.015	0.020	—	0.025	—
prl	0.038	0.023	0.018	0.015	0.033	0.020	0.025
pg	0.145	0.175	0.170	0.130	0.105	0.060	0.045
ms	0.752	0.753	0.747	0.780	0.792	0.830	0.845

Note: Grade 3 is represented by two specimens and grade 8 by one. Value in parentheses is one standard deviation. See text for grade assemblages. Abbreviations (Kretz, 1983): Ba-ms—"Ba-muscovite"; Ti-ms—"Ti-muscovite"; $KTi(Fe,Mg)AlSi_3O_{10}(OH)_2$; phl-ann—phlogopite-annite; ce—celadonite; $KAl(Fe,Mg)Si_4O_{10}(OH)_2$; prl—pyrophyllite; pg—paragonite; ms—muscovite.

metamorphic conditions demonstrates that these assumptions are reasonable.

Muscovite

Analyses for muscovite are provided in Appendix Table 1 and summarized by zone in Table 1. All specimens contain ≤ 0.001 Ca and ≤ 0.004 Mn ions. Based on analyses of 6 specimens over a range of grade, muscovite contains between 0.02 and 0.13 wt% F, corresponding to an average 1.2 ± 1% substitution of OH by F. These values are comparable to those of Evans (1969).

In both muscovite and biotite, all substitutions involve either (1) octahedral sites, (2) octahedral and tetrahedral sites, or (3) tetrahedral and 12-fold sites. Nothing in the analyses suggests the need for any coupled substitutions involving a combination of octahedral and 12-fold sites. The muscovite substitutions can be viewed using the concept of exchange components (Thompson, 1982) with muscovite ($KAl_2AlSi_3O_{10}(OH)_2$) as the additive component.

The octahedral site occupancy of all the muscovites is remarkably constant averaging 4.044 ± 0.012 calculated on a 22-oxygen basis. This suggests that (1) any substitutions involving octahedral vacancies must be nearly constant in amount for all the muscovites and (2) there is a limited and constant amount of trioctahedral substitution. Most studies of muscovite have shown excess octahedral ions (Guidotti, 1984), and in the present muscovite this takes the form of about 2 mol% phlogopite-annite. The substitution involving Ti, since it is variable in extent, cannot involve a change in vacancy content. Holdaway (1980) showed that for pelitic muscovite coexisting with ilmenite and an Al-rich mineral, R^{2+} increases and ^{vi}Al decreases with increasing Ti, with slopes of 0.98 and −2.02, respectively, consistent with the substitution $TiR^{2+}Al_{-2}$. These same relations can be seen in the present data (Table 1) if zones 3 (2 specimens) and 8 (1 specimen) are ignored.

The average end-member muscovite composition of each zone was calculated from the 22-oxygen stoichiometry by first dividing by 2 and then using the following procedure: (1) "Ba-muscovite"[1] = Ba; (2) "Ti-muscovite,"[1] $KTi(Fe,Mg)AlSi_3O_{10}(OH)_2$ = Ti; (3) phlogopite-annite = [Σ(vi) − 2]; (4) celadonite (ce) = {Fe + Mg − Ti − 3[Σ(vi) −2]}; (5) pyrophyllite is the average of [1 − Σ(xii)] and (Si − ce + Ba − 3) (these differ by between 0 and 2.5 mol%); (6) paragonite = Na; (7) muscovite is the remainder. The dominant substitutions in these muscovites are $TiR^{2+}Al_{-2}$ for "Ti-muscovite," $R_3^{2+}Al_{-2}\square_{-1}$ for phlogopite-annite, $R^{2+}SiAl_{-2}$ for celadonite, $\square SiK_{-1}Al_{-1}$ for pyrophyllite, and NaK_{-1} for paragonite.

It should be noted that the celadonite values near 2 mol% are partly a function of the other end members assumed and the sequence in which they were calculated, and partly a function of the standards used for analysis. Because of the inaccuracy of estimating octahedral ions above 2, phlogopite-annite and celadonite contents must have large errors relative to the other components. However, low celadonite contents are reasonable for the pressures at which these muscovites crystallized.

The effects of grade on composition of muscovite are very subtle and approximately the same as those noted by Guidotti for muscovite in comparable assemblages (1978; 1984, p. 407) for the Rangeley area, Maine. Briefly summarized, they are (1) Ti and R^{2+} increase with grade, (2) ^{vi}Al decreases with grade, and (3) paragonite content

[1] "Ba-muscovite," "Ba-biotite," "Ti-muscovite," and "Ti-biotite" are given in quotation marks to emphasize that they are hypothetical end-member components and not mineral names.

TABLE 2. Summary of average biotite stoichiometry by grade, based on 22 oxygens

Grade:	3	4	5	6	6.5	7	8
Si	5.42(0)	5.38(4)	5.38(2)	5.37(1)	5.35(1)	5.34(2)	5.36
^{iv}Al	2.58(0)	2.62(4)	2.62(2)	2.63(1)	2.65(1)	2.66(2)	2.64
^{vi}Al	0.84(4)	0.92(3)	0.90(2)	0.88(10)	0.78(4)	0.79(3)	0.86
Ti	0.18(0)	0.17(2)	0.23(4)	0.25(5)	0.33(4)	0.38(3)	0.33
Fe	2.51(39)	2.52(30)	2.53(15)	2.51(21)	2.55(7)	2.53(6)	2.33
Mg	2.23(42)	2.17(31)	2.07(10)	2.05(21)	1.97(12)	1.85(10)	2.05
Mn	0.02(1)	0.01(1)	0.01(0)	0.01(1)	0.02(0)	0.01(1)	0.01
Σ(vi)	5.78(1)	5.79(5)	5.73(3)	5.71(5)	5.65(4)	5.57(4)	5.59
K	1.74(4)	1.68(7)	1.71(2)	1.74(5)	1.80(5)	1.90(3)	1.86
Na	0.04(2)	0.07(2)	0.07(2)	0.07(1)	0.06(1)	0.03(1)	0.03
Σ(xii)*	1.78(5)	1.76(7)	1.78(2)	1.81(5)	1.82(4)	1.94(2)	1.90
Fe/(Fe + Mg)	0.53(9)	0.54(6)	0.55(3)	0.55(4)	0.57(2)	0.58(2)	0.53
Ba-bt	0.003	0.003	0.003	0.003	0.003	0.003	0.003
Ti-bt	0.090	0.085	0.115	0.125	0.165	0.190	0.165
tlc-mi	0.110	0.120	0.110	0.090	0.070	0.030	0.050
ms	0.015	0.018	0.018	0.019	0.004	0.021	0.035
eas-sid	0.390	0.424	0.414	0.402	0.382	0.353	0.360
won	0.020	0.035	0.035	0.035	0.030	0.015	0.015
phl-ann	0.372	0.315	0.305	0.326	0.346	0.388	0.372

Note: Abbreviations (Kretz, 1983): Ba-bt—"Ba-biotite"; Ti-bt—"Ti-biotite"; $KTi\square(Fe,Mg)AlSi_3O_{10}(OH)_2$; tlc-mi—talc-minnesotaite; ms—muscovite; eas-sid—eastonite-siderophyllite, $KAl(Fe,Mg)_2Al_2Si_2O_{10}(OH)_2$; won—wonesite; phl-ann—phlogopite-annite.

* Includes 0.005 Ba (see text).

first increases and then decreases as grade rises. Most of the changes in muscovite composition reflect the changing saturation levels of "Ti-muscovite" and paragonite content. Several of the most subtle changes seen by Guidotti, e.g., decreasing Σ(vi) and decreasing Si, are not seen in the present muscovites. Differences in average Si content between the two suites clearly reflect differences in standardization for analysis.

Biotite

Microprobe analyses for biotite are provided in Appendix Table 1 and summarized by zone in Table 2. All specimens contain ≤0.001 Ca ions. Ba in representative biotite is about half the amount in coexisting muscovite. The Fe^{3+} contents were not measured, but must be low and nearly constant, and would produce a small amount of ferri-eastonite or oxy-biotite (Dymek, 1983). Analyses of six biotites over a range in grade indicated 0.13 to 0.41 wt% F (about 4 times that of coexisting muscovite), corresponding to an average substitution of 6.9 ± 2.4% F for OH. Values of F for biotites analyzed by Evans (1969) are 0.12 to 0.50 wt%. Munoz and Ludington (1974, 1977) have shown experimentally that Mg-bearing biotite partitions F to a much greater extent than coexisting muscovite.

In biotite the best selection for the additive component is annite. As is the case with all metamorphic biotite (e.g., Dymek, 1983; Guidotti, 1984), octahedral vacancies are common. A plot of Σ(vi) against Ti (Fig. 2) reveals that for the present biotites, most of which coexist with ilmenite, the vacancies are mainly associated with Ti content. The sum of Σ(vi) + Ti for all the biotites is 5.96 ± 0.04. Clearly most or all of the variation in vacancy content is a linear function of Ti. The relevant substitution is $Ti\square R^{2+}_{-2}$, the most important Ti substitution proposed by Dymek (1983). (The remaining 0.04 units of vacancy may be explained by an average muscovite content of 2 mol%.) The end member associated with Ti substitution is $KTi\square(Fe,Mg)AlSi_3O_{10}(OH)_2$, the same as the "Ti-muscovite" end member. However, in biotite the ions could be disordered over both the M(1) and M(2) sites, whereas in muscovite they are presumably all at M(2) sites.

The combination of 12-fold site vacancies and consistently lower values for (^{iv}Al − 2) than for ^{vi}Al indicates the presence of significant amounts of talc-minnesotaite component in the biotite. The average end-member composition of each zone was calculated from the 22-oxygen stoichiometry assuming 0.005 Ba ions, dividing by 2, and using the following procedure: (1) "Ba-biotite" = Ba; (2) "Ti-biotite" = Ti; (3) talc-minnesotaite = [1 − Σ(xii)]; (4) muscovite = the average of [3 − Σ(vi) − Ti] and ½[^{vi}Al − ^{iv}Al + Σ(xii)] (these differ by ≤1 mol%); (5) eastonite-siderophyllite = (^{vi}Al − 2ms); (6) wonesite = Na; (7) phlogopite-annite comprises the remainder. The dominant substitutions in these biotites are $Ti\square R^{2+}_{-2}$ for "Ti-biotite," $\square SiK_{-1}Al_{-1}$ for talc-minnesotaite, $Al_2\square R^{2+}_{-3}$ for muscovite, $Al_2R^{2+}_{-1}Si_{-1}$ for eastonite-siderophyllite, and NaK_{-1} for wonesite. This procedure is comparable to that used by Dymek (1983) except that Dymek's more oxidized rocks necessitated an attempt to calculate Fe^{3+} values, whereas the reasonable assumption of zero Fe^{3+} content for these biotites makes the procedure simpler and perhaps more accurate.

The effects of grade on composition of biotite are more noticeable than those for muscovite and are essentially the same as those observed by Guidotti (1984, p. 446). In summary, the changes with grade are (1) slight decrease in Si and corresponding increase in ^{iv}Al, (2) de-

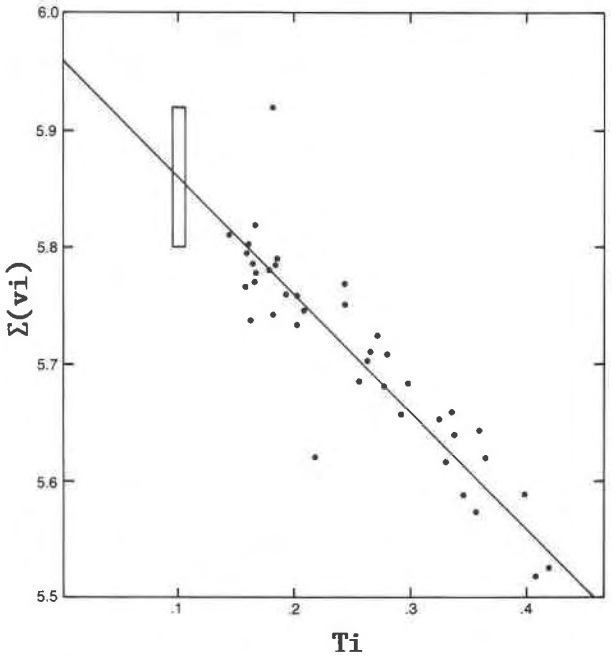

Fig. 2. Plot of Σ(vi) vs. Ti in ions per 22-oxygen formula unit for biotites. The average sum of Σ(vi) + Ti is 5.96 ± 0.04. The line is drawn through this intercept with a slope of −1 indicating that most of the Ti substitution in biotite is charge-balanced by vacancies in the octahedral layer. Box is estimated (1σ) analytical precision.

crease in ^{vi}Al, (3) a pronounced increase in Ti and corresponding decrease in Σ(vi), (4) an increase in Σ(xii), and (5) a slight increase in Fe/(Fe + Mg). These changes with grade primarily reflect a progressive increase in "Ti-biotite" and progressive decreases in talc-minnesotaite and eastonite-siderophyllite as grade increases.

Several of the highest-grade rocks contain little or no ilmenite. Biotite in grade 7 of the Maine rocks (Fig. 1) contains an average of 19 mol% "Ti-biotite." Biotite analyzed by Tracy (1978) from ilmenite-bearing rocks of the Quabbin Reservoir area, Massachusetts, also contains 19% "Ti-biotite" on the average. It appears that despite absence of ilmenite in some rocks, the biotite from Maine is essentially saturated with respect to Ti. Also the Quabbin Reservoir rocks, which probably formed at somewhat higher P, do not appear to have formed at higher T or they would have had higher Ti in biotite coexisting with ilmenite. The explanation may lie in the fact that high-grade rocks in both areas appear to involve vapor-absent partial melting of muscovite-bearing pelites. According to Kerrick (1972), this melting should occur at a nearly constant T over a P range of several kilobars.

The increase in average Fe/(Fe + Mg) followed by a possible decrease at the highest grades results from the interplay of two factors: (1) The reactions summarized by Holdaway et al. (1982) for these rocks (Fig. 3) imply an increase in Fe/(Fe + Mg) as Fe-rich staurolite reacts away and then Fe-rich garnet partially reacts with muscovite, but at the highest grades (7, 8) biotite starts to react with sillimanite to grow more Fe-rich garnet and K-feldspar thus reducing Fe/(Fe + Mg) in biotite (Thompson, 1976). (2) As grade increases, biotite and garnet must move closer together in Fe/(Fe + Mg) ratio as a consequence of the T effect on the garnet-biotite exchange reaction (Ferry and Spear, 1978).

Garnet

Stoichiometry of the cores and intermediate zones of garnets is provided in Appendix Table 1 and summarized by grade in Table 3. Compositional changes of garnets with grade are as follows: (a) almandine and pyrope contents first increase while staurolite is present (grades 4, 5), then decrease as garnet begins to react (grades 6, 6.5), and then increase again with the onset of new growth (grades 7, 8); (b) spessartine content behaves opposite to almandine and pyrope; (c) grossular content remains more or less constant at about 4 mol%; (d) Fe/(Fe + Mg) decreases with increasing grade. Zoning in garnet is characterized (a) by a slight outward decrease in Fe/(Fe +

TABLE 3. Summary of average garnet stoichiometry by grade

Grade:	3	4	5	6	6.5	7	8
			Core				
alm	0.60(7)	0.71(8)	0.74(4)	0.68(5)	0.70(1)	0.74(4)	0.70
prp	0.06(2)	0.09(2)	0.10(1)	0.10(2)	0.11(1)	0.12(1)	0.18
sps	0.29(6)	0.15(7)	0.12(4)	0.17(3)	0.16(2)	0.10(5)	0.06
grs	0.04(1)	0.05(2)	0.04(2)	0.04(2)	0.03(1)	0.03(2)	0.06
Fe/(Fe + Mg)	0.90(4)	0.89(2)	0.88(1)	0.87(3)	0.86(1)	0.86(1)	0.80
			Intermediate zone				
alm	0.68(12)	0.73(7)	0.75(4)	0.70(5)	0.71(1)	0.74(4)	0.72
prp	0.08(1)	0.09(2)	0.10(1)	0.10(2)	0.11(1)	0.11(1)	0.16
sps	0.19(12)	0.13(6)	0.12(4)	0.16(4)	0.15(2)	0.11(4)	0.06
grs	0.04(1)	0.05(2)	0.04(2)	0.04(2)	0.03(1)	0.03(2)	0.06
Fe/(Fe + Mg)	0.89(3)	0.89(2)	0.88(2)	0.88(2)	0.87(1)	0.87(0)	0.82
T*	pro.	pro.	retro.	retro.	retro.	retro.	retro.

Note: Abbreviations (Kretz, 1983): alm—almandine; prp—pyrope; sps—spessartine; grs—grossular.

* Based on average garnet-biotite temperatures (Table 8), intermediate zones are designated progressive or retrogressive.

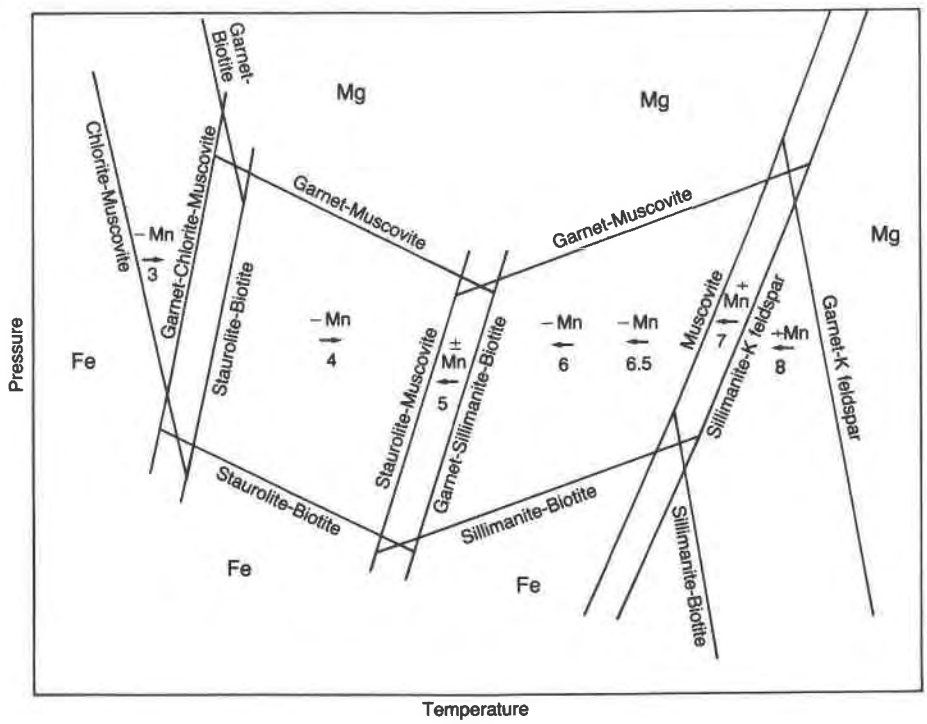

Fig. 3. Tentative *P-T* diagram showing divariant reactions involving garnet in pelitic rocks. Lower curves are Fe end-member boundaries, and upper curves are Mg end-member boundaries. The three AFM model univariant curves are also shown as narrow divariant fields. Numbers represent grade designations for M_3 and M_5, ±Mn indicates increase or decrease in Mn from core to intermediate zone of garnet, and arrow indicates increase or decrease in *T* from core to intermediate zone. The signs of slopes are consistent with observations on M_3 and M_5 metamorphism. At high or low *P*, signs of slopes may change (e.g., Spear and Selverstone, 1983). Within the wide fields, the divariant reaction is the only reaction involving Fe-Mg components. The tentative conclusion that prograde chlorite disappears early in the staurolite zone is discussed in the section on chlorite mineral chemistry and petrologic interpretation.

Mg) at garnet and staurolite grades (3, 4) and a slight outward increase in Fe/(Fe + Mg) in all successive grades and (b) by spessartine content decreasing outward in grades 3 and 4, remaining nearly constant in grade 5, decreasing outward in grades 6 and 6.5, and increasing outward in grades 7 and 8.

Prograde changes in garnet composition. The steady change in average Fe/Mg ratio of garnet with grade can be seen in the cores, the intermediate zones, and even in the peak metamorphic portion of the garnet (the intermediate zone for grades 3 and 4 and the core for higher grades). With increasing *T*, the garnet moves compositionally closer to the biotite (K_D approaches unity) as a consequence of the *T* effect on the garnet-biotite exchange reaction (Ferry and Spear, 1978).

The progressive changes in average Mn content are explained in Figure 3. Because garnet is the only Mn-rich phase in the rocks, Mn content of garnet is an especially good monitor of growth or reaction. Garnet decreases in Mn as it grows at garnet and staurolite grades (3, 4). When garnet reaches staurolite-sillimanite grade (5), it has reached a minimum Mn content relative to adjacent grades 4 and 6. Once staurolite disappears, Mn content increases in grade 6 as garnet and muscovite react. The lower average Mn content of grades 6.5 and 7 is inconsistent with the garnet-muscovite reaction, which should increase Mn. In the narrow *T* range of zone 7, a simple *T* increase should leave the average garnet more or less unchanged while muscovite and K-feldspar adjust their Na content. The lower Mn content of grades 6.5 and 7 is a problem that can be most easily explained by a higher *P* of crystallization for these rocks (Fig. 3) than for grades 3 to 6. The rocks of grades 6.5 and 7 are not only the southernmost rocks of the region, but they were metamorphosed during the younger M_5 event. A single rock in zone 8 has still lower Mn in the garnet, but this can be explained in part by the reaction of biotite and sillimanite to garnet and K-feldspar in a rock where most of the muscovite has reacted away.

Garnet zoning. Most garnets are zoned continuously from core to rim. The compositional behavior of zoned garnets (Table 3) can be explained with the aid of Figure 3 and the garnet-biotite temperatures (details in a subsequent section; see Table 8). Garnet-biotite geothermometry demonstrates that at garnet and staurolite grade (3, 4), garnet zoning is mainly of a prograde nature, reflecting a temperature increase, whereas at higher grades, the zoning is dominantly retrograde with the intermedi-

TABLE 4. Summary of average staurolite and chlorite stoichiometry by grade

	Staurolite			Chlorite	
Grade	4	5		3	4
Si	7.62(6)	7.64(11)	Si	5.19(5)	5.14(2)
^{iv}Al	0.38(6)	0.36(11)	^{iv}Al	2.81(5)	2.86(2)
^{vi}Al	17.53(1)	17.53(4)	^{vi}Al	2.92(6)	2.93(3)
Ti	0.10(1)	0.11(1)	Ti	0.01(0)	0.01(1)
Fe	3.31(18)	3.09(37)	Fe	4.46(81)	4.60(62)
Mg	0.60(10)	0.53(9)	Mg	4.48(83)	4.36(65)
Mn	0.06(4)	0.07(2)	Mn	0.04(3)	0.02(2)
Zn	0.09(8)	0.18(14)	Ca	0.00(0)	0.00(0)
Li*	[0.31]	[0.51]	Σ(vi)	11.90(0)	11.93(2)
H	[2.97]	[3.04]	Fe/(Fe + Mg)	0.050(9)	0.51(7)
$\Sigma(R^{2+} + Li + H)$*	5.86(4)	5.91(17)			
Fe/(Fe + Mg)	0.85(2)	0.86(1)			

Note: See text for calculation of stoichiometry of staurolite. Error in ^{vi}Al is artificially low because of this procedure. Brackets indicate that these entries are based mainly on estimated values.

* For analyses for which Li_2O was not determined, Li is estimated as 0.3 atoms (see App. Table 1).

ate zone of the garnet indicating a lower temperature than the core. A decrease in Mn content of the garnet from core to intermediate zone indicates that the garnet was growing (growth zoning), and an increase in Mn content indicates that the garnet underwent late-stage resorption or diffusion zoning (Tracy, 1982).

Growth zoning is indicated in grades 3 and 4 where increasing T coincides with decreasing Mn. Garnet grew first in response to reaction of chlorite to garnet in the garnet zone and then as staurolite-biotite reacted to almandine-muscovite in the staurolite zone. The consistent decrease in Mn in zoned garnets of the staurolite zone is supporting evidence that the staurolite-biotite to garnet-muscovite equilibrium has a negative slope (see also Holdaway et al., 1982). This reaction was probably not affected by traces of chlorite in several staurolite-grade rocks, because the chlorite is believed to be retrograde, as discussed below. At staurolite-sillimanite grade (5), the constancy of Mn indicates that garnet was neither being created nor destroyed, but the intermediate zones of garnet generally equilibrated at lower temperatures than the cores (see Table 8).[2] This diffusion zoning must have been produced in a retrograde fashion with biotite and sillimanite tending to react to garnet, but with slight staurolite production consuming garnet (Fig. 3). In grades 6 and 6.5, decrease of Mn with decreasing T in the garnets indicates a retrograde growth zoning (Cygan and Lasaga, 1982). Retrograde reaction of biotite and sillimanite to garnet and muscovite accounts for the Mn decrease. In grades 7 and 8, increase of Mn with decreasing T (diffusion zoning) results from decrease in garnet content as it reacts with K-feldspar during the early stages of cooling.

[2] Retrograde zoning in grade 5 is partly an artifact of the fact that biotite used for core *and* intermediate-zone T calculation is the same final biotite. For grades 3 to 6, Fe/(Fe + Mg) in biotite increases 0.02 mol%/K (Tables 2, 8). Less than half of the garnet re-equilibrated with biotite during the (average) 15 °C retrogression. Thus, biotite changed about −0.15 mol%, indicating that actual T values for grade 5 cores were about 2 °C lower than measured (Ferry and Spear, 1978).

Staurolite

Of the 16 staurolite specimens analyzed in this study (App. Table 1, App. 1, and Table 4), 4 were analyzed for H_2O (Holdaway et al., 1986c) and 3 were analyzed for Li_2O (Dutrow et al., 1986). Holdaway et al. (1986b) showed that, for a larger group of complete staurolite analyses, (Si + Al) was nearly constant on a 48-oxygen basis: for 31 staurolites, (Si + Al) = 25.43 ± 0.13; for 28 of these 31 staurolites not containing high Fe^{3+}, (Si + Al) = 25.46 ± 0.09; and for 6 Maine specimens that all formed under reducing conditions with graphite, (Si + Al) = 25.53 ± 0.03. In order to produce a stoichiometry that is both accurate and consistent with those specimens analyzed for water, we normalized the stoichiometry of the 12 specimens not analyzed for H_2O and Li_2O to 25.53 (Si + Al). The total positive charge was then subtracted from 96 to give an approximation of the (H + Li) ions. Through a propagation of errors it was determined that the approximate (H + Li) content has an error (1σ) of ±0.3 ions. Based on the Li analyses of five specimens from Maine, the average number of Li ions for the remaining staurolites can be estimated at 0.3, allowing for reasonable estimates of H ions that agree well with those analyzed for water.

The overall stoichiometry of the staurolite agrees very well with that given for the 31 staurolites by Holdaway et al. (1986b). Mn and Ti are consistently low, whereas Zn and Li are somewhat variable. This variability becomes more apparent in the specimens from grade 5 where staurolite was breaking down by reaction with muscovite and quartz to sillimanite, garnet, and biotite (e.g., Guidotti, 1974). The most unusual staurolite is specimen 6 from near East Winthrop (Fig. 1). This staurolite forms about 1% of the rock but occurs in small euhedral crystals rather than as remnants in mica pseudomorphs, the more common occurrence of the mineral as it reacts out (Holdaway et al., 1982; Guidotti, 1968). It may have been stabilized by the ~1 Li ion per 48 oxygen (see also Dutrow et al., 1986).

Based in part on the structure determination of Smith

(1968), Holdaway et al. (1986b) suggested that 0.25 Fe^{3+} ions be assigned to staurolite Al octahedral sites, 0.25 (Mn + Fe^{2+}) be assigned to U sites, and the remaining Fe, Mg, Zn, Li, Ti, and vacancies be assigned to the four tetrahedral sites, allowing for the determination of an approximate activity model. Because the present staurolites grew under more reducing conditions than the average staurolites used for H_2O analyses and structure determinations, it is reasonable to assume that, for the present staurolite, about 0.15 rather than 0.25 Fe^{3+} replace octahedral Al and the remaining Fe is Fe^{2+}. This value is approximately equal to the lowest Fe^{3+} determinations of Juurinen (1956).

Values of Fe/(Fe + Mg) for staurolites range from 0.81 to 0.89. Staurolites show no zoning and no consistent pattern of compositional change with grade. If the Li-rich specimen is discarded, the other four staurolites from grade 5 range from 0.849 to 0.853, averaging 0.851 ± 0.002, suggesting that the staurolite breakdown approximates a univariant reaction.

As shown in Figure 4, the staurolite-biotite K_D is apparently unaffected by grade whereas the average staurolite-garnet K_D appears to increase slightly from grade 4 to grade 5. Specimen 6 exhibits anomalous K_D values, i.e., the staurolite Fe/(Fe + Mg) is about 7 mol% more Fe-rich than would be indicated by the biotite and garnet compositions in the specimen. Apparently the effect of high Li on staurolite is to impose a positive deviation from ideality on the Fe-Mg solid solution or increase possible Fe-Mg immiscibility. Holdaway et al. (1986b) suggested that for a given P and T, there are limits on the amount of smaller ions (Zn, Mg, Li, and Ti) that the tetrahedral Fe sites can hold. An increase in Li must decrease the maximum possible amount of Mg, other things being equal. This phenomenon is also shown by increasing Li with increasing Fe/Mg in staurolite (Dutrow et al., 1986, Fig. 4).

In both the biotite and garnet K_D plots there is a tendency for Mg-rich staurolite to exhibit a slightly higher K_D than more Fe-rich staurolite. As Mg content increases, the Fe/(Fe + Mg) of staurolite is slightly higher than would be predicted from ideal solid solution, indicating positive deviation from ideality in staurolite (assuming that the biotite and garnet Fe-Mg solid solutions are close to ideal). If some of the Fe is subtracted from staurolite Fe values to account for the minor U-site and octahedral Al–site occupancy as discussed above, the absolute K_D values are changed somewhat, but the relationships remain the same. Zn and Li contents of most of the staurolites are low enough to have no measurable effect on K_D.

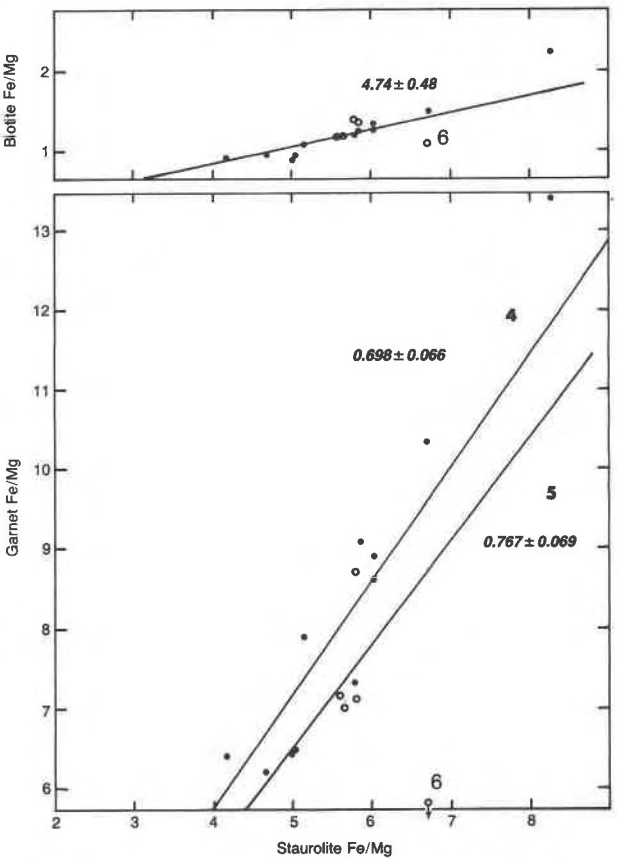

Fig. 4. K_D Fe-Mg plots for staurolite-biotite and staurolite-garnet (using peak metamorphic zone of garnet). Dots represent grade 4 and circles represent grade 5. Specimen 6, Li-rich staurolite, is identified, and plots at garnet Fe/Mg = 4.07. Lines give average K_D for staurolite-biotite and average K_D by grade (designated as 4 or 5) for staurolite-garnet, excluding specimen 6. Average K_D and standard deviation are given.

Chlorite

Chlorite is an important mineral in garnet-grade (3) rocks, but forms only <2% of 8 of 11 analyzed staurolite-grade (4) rocks. Only well-crystallized chlorite, not seen replacing biotite, garnet, or staurolite, was chosen for analysis (App. Table 1; Table 4). One exception to this is in specimen 94 where chlorite discontinuously surrounds and partly replaces staurolite. Simple stoichiometry involving Si, Al, Mg, Fe, and minor Mn characterizes the chlorites. The numbers of Al and Si ions are very nearly constant for Al-saturated rock compositions and resemble those reported by Novak and Holdaway (1981), Guidotti (1974), and Dutrow (1985) for chlorites of graphite-bearing pelites from Maine. The present chlorites and those of Novak and Holdaway (1981), using a different microprobe and standards, show 0.086 ± 0.041 higher ^{vi}Al than ^{iv}Al and slightly low Σ(vi). To a lesser degree, the same tendency is seen in the data of Guidotti (1974). These observations cannot be explained by Fe^{3+} substituting for ^{vi}Al or by intercalated biotite, talc, or wonesite layers (Veblen, 1983) because all these effects tend to increase octahedral R^{3+} or increase Si, which would also increase apparent octahedral Al.

Three possible explanations for these observations are suggested. (1) They may result from a calibration error in microprobe analyses of about 1% relative for SiO_2 or

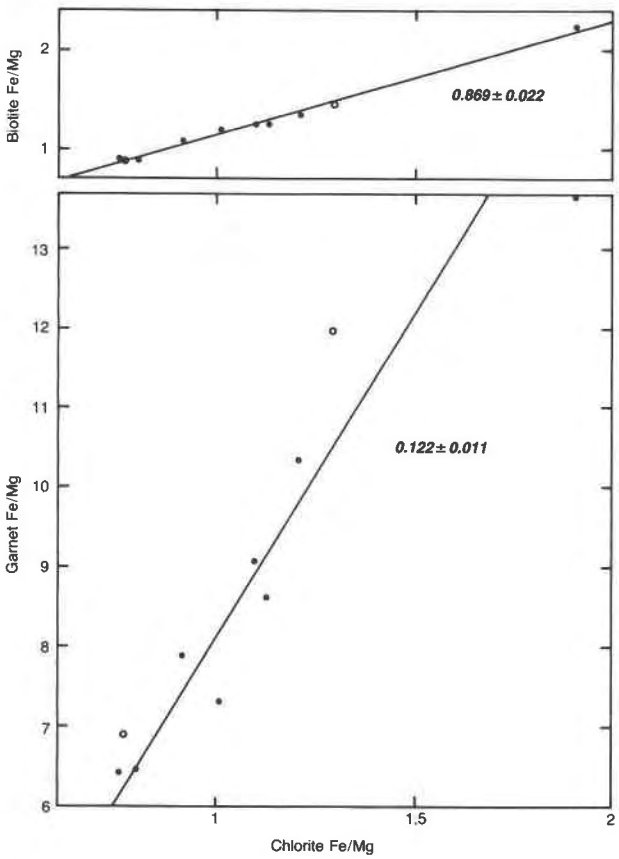

Fig. 5. K_D Fe-Mg plots for chlorite-biotite and chlorite-garnet (using peak metamorphic zone of garnet). Circles represent grade 3 and dots represent grade 4. Lines represent average K_D. Average K_D and standard deviation are given.

Al_2O_3. Although correcting for such an error would bring ^{vi}Al and ^{iv}Al into agreement, it would lower Σ(vi) still more. (2) The total number of anions per formula unit may not be stoichiometric. Specifically, the chlorite may contain a few percent of intercalated brucite layers (Veblen, 1983, p. 574). To allow for extra brucite layers, the oxygen basis needs to be increased slightly from 28, which would also increase Σ(vi). (3) The chlorite may contain very limited dioctahedral substitution (Eggleston and Bailey, 1967; Tompkins et al., 1984). In the absence of TEM work it is impossible to distinguish between these last two possibilities.

The main compositional variation in chlorite is in Fe/Mg ratio. Garnet-chlorite K_D varies with grade, whereas biotite-chlorite K_D appears to be constant (Fig. 5). The recently calibrated garnet-chlorite geothermometer (Dickenson and Hewitt, 1986) gives temperatures that average about 5 °C below those of the Ferry and Spear (1978) garnet-biotite geothermometer (Table 5), suggesting that garnet-chlorite K_D gives a reasonable estimate of prograde T in these rocks.

The AFM univariant assemblage staurolite-garnet-biotite-chlorite-muscovite-quartz occurred over a T interval of about 50 °C. In rocks such as these, in which P, X_{H_2O}, and f_{O_2} were nearly constant, one might expect significant variations in non-AFM components in one or more minerals to allow for this assemblage to exist over such a T range. Such variations are not seen, and the variations that do occur are random in nature or easily explained by other reactions (see App. Table 1). A number of arguments based on the present work and observations elsewhere suggest that many of the chlorites in the rocks of grade 4 are retrograde and result from minor reaction of biotite and other minerals to chlorite: (1) Biotite coexisting with staurolite and prograde chlorite should have a restricted range of Fe/(Fe + Mg) that should be *lower* than that ratio in rocks containing stauro-

TABLE 5. Comparison of garnet-chlorite and garnet-biotite temperatures; calculated equilibrium constants for Reaction 1

Grade	Specimen	Temperature (°C) C**	C†	I**	I†	ln K^*
3	2	461	467	470	477	0.366
3	96	442	443	461	460	0.214
4	52	455	470	480	494	0.503
4	3	484	499	484	499	0.526
4	61	500	498	495	494	0.433
4	84	484	481	484	481	0.252
4	129	494	497	483	486	0.378
4	114	520	513	507	501	0.469
4	94	537	544	537	544	0.378
4	27	527	534	541	546	0.302
Average		490 ± 32	495 ± 31	494 ± 27	498 ± 27	0.382 ± 0.104

Note: Sequence is that of increasing T given in Appendix Table 1, based on Table 8. Abbreviations: C = core; I = intermediate zone.

* Approximate equilibrium constant; values of ln K^* for Reaction 1 using activity models given in text.

** Temperature based on garnet-biotite compositions and Dickenson and Hewitt (1986) geothermometer modified by M. P. Dickenson (pers. comm., 1987).

† Temperature based on garnet-biotite geothermometry (Table 8). Ferry and Spear (1978) calibration was used because the garnet-chlorite geothermometer was calibrated with Ferry and Spear (1978).

lite-biotite without chlorite (e.g., see AFM diagram of Guidotti, 1974). In grade 4 biotites, Fe/(Fe + Mg) ranges from 0.47 to 0.69 in chlorite-bearing rocks, and from 0.47 to 0.57 in rocks without chlorite. Small differences in X_{H_2O} of the fluid phase could account for some variability but are unlikely to produce the observed degree of randomness during *prograde* metamorphism. (2) If chlorite and garnet were an equilibrium pair in the present rocks, then the Fe end-member equilibrium (Reaction 1) with T (Fig. 5). The composition of retrograde chlorite is controlled by the dominant biotite in the rock and the chlorite-biotite K_D. In M_2 (Dickerson, 1984), retrograde chlorite is widespread, and almost all chlorite is clearly retrograde. Here the chlorite-biotite K_D is 0.858 ± 0.040 compared with 0.869 ± 0.022 for the present rocks. The close compositional relationship between chlorite and biotite is maintained despite the widespread retrogression in M_2.

$$\underset{\text{Chlorite}}{0.250Fe_{4.51}Al_{1.47}(Al_{1.43}Si_{2.57})O_{10}(OH)_8} + \underset{\text{Muscovite}}{0.010K_{0.97}Al_{1.92}Fe_{0.12}(Al_{0.97}Si_{3.03})O_{10}(OH)_2} + \underset{\text{Quartz}}{0.458SiO_2}$$

$$= \underset{\text{Almandine}}{0.367Fe_3Al_2Si_3O_{12}} + \underset{\text{Biotite}}{0.011K_{0.88}Fe_{2.53}Al_{0.47}(Al_{1.31}Si_{2.69})O_{10}(OH)_2} + \underset{\text{Fluid}}{H_2O} \quad (1)$$

would apply to all rocks of grades 3 and 4 that contain chlorite. Approximate mineral equilibrium constants (K^*) were calculated to take into account dilution of Fe and K by other components, assuming that Al varies little from the average amounts (Tables 1–4). Activity models based on mineral compositions in Reaction 1 are as follows:

$$\begin{aligned}
&\text{Chlorite} && a_{FeChl} = [Fe/(Fe + Mg + Mn)]^{4.51}\\
&\text{Muscovite} && a_{Mus} = [K/(K + Na)]^{0.97}[Fe/(Fe + Mg)]^{0.12}\\
&\text{Almandine} && a_{Alm} = (X_{Fe}^{Grt})^3\\
&\text{Biotite} && a_{FeBt} = [K/(K + Na)]^{0.88} \times\\
& && \quad [Fe/(Fe + Mg + Mn + 2Ti)]^{2.53}.
\end{aligned}$$

The calculated values of K^* are given in Table 5 in order of increasing T (based on Table 8). The relation between K^* and T for an equilibrium reaction (Kerrick, 1974) is

$$\Delta T = RT_r^2 \ln(K^* a_{H_2O}^n)\Delta S_r^{-1}. \quad (2)$$

Thus as T increases and ΔT rises relative to the equilibrium T calculated for the end-member reaction (e.g., Fig. 3), ln K^* must increase if equilibrium prevails. It is clear that prograde T is not the controlling factor for K^*. Variation in K^* can result from changes in the H_2O activity as shown by Equation 2, but in reduced graphitic rocks, such variation is not expected to exceed 15% (e.g., see Table 12), leading to a maximum variation of 0.16 in ln K^*. With the possible exception of the first four specimens listed in Table 5, K^* for Reaction 1 does not support chlorite as an equilibrium prograde mineral in the staurolite zone. (3) Chlorite occurs as small amounts of well-crystallized grains of variable size mainly cross-cutting the foliation defined by muscovite and some of the biotite. It commonly occurs near porphyroblasts of staurolite or biotite. (4) Aluminum silicate and Mg-bearing biotite are a common *lower* staurolite-zone assemblage elsewhere, suggesting that the alternative staurolite-chlorite assemblage becomes unstable early in the staurolite zone. Examples are M_2 in Maine where under reducing conditions, andalusite-biotite becomes stable immediately after staurolite (Dickerson and Holdaway, ms.); the Picuris Mountains in New Mexico where andalusite-biotite and sillimanite-biotite occur next to normal lower staurolite–grade rocks (Holdaway, 1978); and the Snake Range, Nevada, where kyanite-biotite occurs above normal staurolite-grade rocks in a sequence of downward-increasing grade (Geving, 1987).

One important question remains to be answered: If much of the chlorite of grade 4 is retrograde, why does it give reasonable T values with the garnet-chlorite geothermometer (Table 5)? The answer apparently lies in the constancy of chlorite-biotite K_D

Based on these observations, we tentatively conclude that much of the chlorite in grade 4 grew from biotite and other minerals during cooling or M_5 reheating of the rocks at temperatures in the range of 450–500 °C and perhaps at pressures higher than those of M_3. Equilibrium retrograde domain assemblages must have been garnet-chlorite-staurolite-biotite, garnet-chlorite-staurolite, garnet-chlorite-biotite, and staurolite-chlorite-biotite (all assemblages containing muscovite + quartz). This conclusion suggests a re-evaluation of the first sillimanite-forming reaction proposed by Guidotti (1974) for the Rangeley area on the western side of the present study area and by Holdaway et al. (1982) for the present area. Instead of staurolite-chlorite-muscovite reacting to sillimanite-biotite in normal M_3 rocks, we suggest that staurolite-muscovite reacted to sillimanite-biotite-garnet. The chlorite-staurolite tie line in AFM projection must break immediately after staurolite forms, allowing garnet-chlorite-staurolite-biotite to exist over a limited T range, consistent with the high ΔS involved in chlorite dehydration. The staurolite-grade (4) M_3 rocks of Maine occupy narrow compositional and pressure ranges such that neither aluminum silicate[3] nor chlorite occur as equilibrium prograde minerals. At lower P during M_2, staurolite was more Fe-rich and occurred with andalusite over a range of grade as indicated by field relations (Dickerson and Holdaway, ms.). At this lower P the common bulk compositions intersect the AFM fields of staurolite-biotite-garnet and staurolite-biotite-andalusite.

Ilmenite

The only significant components detected in ilmenite were Fe, Ti, and Mn (App. Table 1; Table 6). Ilmenite content varies from 89 to 99%, pyrophanite ($MnTiO_3$) from 1 to 11%, and hematite from 0 to 4%. The only obvious compositional pattern is a strong tendency for the pyrophanite content to mirror spessartine content of the garnet. The lower Mn in the ilmenite combined with much lower ilmenite content than garnet in the rocks indicates that only a few percent of the Mn in the rocks is contained in ilmenite and most remaining Mn occurs in garnet.

[3] But see Note added in proof.

TABLE 6. Summary of average ilmenite composition by grade

Grade	3	4	5	6	6.5
ilm	0.94(5)	0.97(2)	0.96(2)	0.94(4)	0.95(1)
pyr	0.06(5)	0.03(2)	0.04(2)	0.05(3)	0.04(2)
hem	0.00(0)	0.01(1)	0.00(0)	0.01(1)	0.01(1)

Note: Abbreviations (Kretz, 1983): ilm—ilmenite; pyr—pyrophanite ($MnTiO_3$); hem—hematite.

Careful inspection of polished sections of grades 6.5 to 8 shows that most of the opaque grains are graphite. In several specimens, no ilmenite was detected; and in others, only trace amounts were seen (see App. Table 1). This scarcity of ilmenite is not related to Fe/(Fe + Mg) of biotite, nor is rutile present in any of the specimens. Presumably, low ilmenite content results from increased Ti solubility in biotite at high grades. The most hematite-rich ilmenite (4% in specimen 63) coexists with a trace of graphite. Although graphite is difficult to recognize because of fine grain size in some lower-grade specimens, its obvious presence in all high-grade specimens combined with the low hematite content of all the ilmenite implies that graphite is present in all specimens.

On the basis of 2 (Fe,Ti,Mn,Mg) cations, five ilmenites contain more than 1.01 Ti atoms. The theoretical limit of Ti ions in ilmenite is 1.00 since the larger octahedral sites presumably exclude Ti. Ti ions range from 1.013 to 1.028, and oxide totals range from 97.36 to 98.54%. The remaining ilmenites have oxide totals (corrected for Fe_2O_3 on basis of hematite content) ranging from 98.49 to 100.97%. These results suggest that some element may not have been analyzed in the anomalous specimens. Specimens 6 and 14, the two most extreme cases, were examined semiquantitatively with the ion microprobe. The results (Table 7) indicate that no other ion is present in significant amounts. The high Li of the staurolite in specimen 6 is reflected by 167 ppmw of Li in the coexisting ilmenite. A microprobe wavelength scan of ilmenite in specimen 6 revealed only Ti, Fe, and Mn. Therefore, high stoichiometric content of Ti is probably an artifact of the analysis procedure (small grain size, conduction, thickness of carbon coat, etc.).

TABLE 7. Semiquantitative ion-microprobe analyses of two ilmenites from grade 5

Element	Sample 14	Sample 6
^{7}Li	5.4	167
^{9}Be	1.0	0.2
^{11}B	1.7	0.6
^{23}Na	21	52
^{24}Mg	281	195
^{27}Al	554	282
^{28}Si	804	466
^{39}K	165	170
^{40}Ca	7	34
^{45}Sc	30	55
^{46}Ti	[31.58%]	[31.58%]
^{51}V	100	85
^{52}Cr	18	20
^{54}Fe	36.23%	37.83%
^{55}Mn	3.15%	3.67%
^{88}Sr	1	10
^{93}Nb	227	61

Note: Analyses were normalized to Ti = 31.58%. Analyses are upper limits because background measurements were not made. True values are probably between 0.5 and 2 times the recorded values because of matrix-dependent effects. Unless specified as percent, values are given as parts per million (by weight).

Other analyzed minerals

Plagioclase is commonly observed in rocks of grades 5 and higher (see App. Table 1) and is present in small amounts at lower grades. It is An_{39} in one specimen of grade 5, An_{17-39} in grade 6, An_{16-27} in grade 6.5, and An_{12-53} in grades 7 and 8. The two most calcic compositions, An_{48} and An_{53}, suggest partial removal of albite component through reaction with muscovite (Tracy, 1978).

Orthoclase in grades 7 and 8 varies from Or_{84} to Or_{90} (see App. Table 1). These feldspars are comparable in composition to those of the southwest part of the study area analyzed by Guidotti et al. (1973), e.g., Or_{82} to Or_{90} in grade 7 schists. Celsian content of alkali feldspars averages about 1 mol%.

Most sillimanite coarse enough for analysis is from grades 7 and 8. Analyses of sillimanite from six specimens show no more than trace amounts of Mg, Ti, and Mn, and 0.19 to 0.35 wt% Fe_2O_3. The average content of Fe_2O_3 is 0.27% corresponding to 0.005 Fe atoms per formula. This amount of Fe is of no consequence in calculating reaction boundaries from experimental equilibria.

CONDITIONS OF METAMORPHISM

Metamorphic conditions were deduced on the basis of (1) estimates of metamorphic temperatures by garnet-biotite geothermometry, (2) metamorphic pressure estimates by comparison of the andalusite-sillimanite phase diagram (Holdaway, 1971) with garnet-biotite geothermometry (grades 5 and 6 of M_3), and (3) estimates of pressure for grades 6.5 and 7 of M_5 based on calibration of the muscovite-almandine-biotite-sillimanite (MABS) geobarometer using the results of (2) above. Finally, P and T estimates for grades 5 and 7 were compared with dehydration equilibria in order to test for accuracy and evaluate fluid-composition models.

Geothermometry

The only reasonably well calibrated geothermometer applicable to medium- and high-grade pelitic metamorphic rocks is that based on the garnet-biotite exchange reaction. This geothermometer is ideal for the M_3 and M_5 Maine rocks because the biotite/garnet ratio is high and evidence for extensive retrogressive effects is virtually absent. Table 8 provides garnet-biotite temperatures for garnet core or intermediate zones and surrounding biotite grains not in physical contact with the garnet, using four recent quantitative calibrations: (1) Ferry and Spear (1978), (2) Hodges and Spear (1982), (3) Ganguly and Saxena (1984, 1985), and (4) Ganguly and Saxena (1984, 1985) with ΔW_{Mn} reduced from 3000 ± 500 to 2500 cal.

TABLE 8. Garnet-biotite temperatures (°C)

No.	Ferry-Spear C	Ferry-Spear I	Hodges-Spear C	Hodges-Spear I	Ganguly-Saxena C	Ganguly-Saxena I	Ganguly-Saxena* C	Ganguly-Saxena* I	Peak *T*
				Grade 3 (M_3)					
2	467	477	481	490	535	531	506	*506*	506
96	443	460	462	479	515	525	494	*507*	507
Avg.	455(18)	469(12)	472(13)	485(8)	525(14)	528(4)	500(8)	507(1)	507(1)
				Grade 4 (M_3)					
1A	431	492	465	521	503	522	479	*508*	508
52	470	494	488	509	513	519	498	*508*	508
3A	499	499	513	513	523	523	508	*508*	508
61A	498	494	514	510	534	527	*515*	510	515
84**	481	481	493	493	540	540	521	*521*	521
129**	497	486	518	509	534	515	*525*	509	525
114	513	501	537	524	531	520	*528*	517	528
5A	526	531	553	557	559	560	543	*544*	544
65**	502	518	528	545	546	554	534	*545*	545
94	544	544	564	564	568	568	557	*557*	557
27	534	546	544	555	583	589	576	*584*	584
Avg.	500(32)	508(23)	520(30)	527(24)	539(24)	540(25)	526(27)	528(26)	531(24)
				Grade 5 (M_3)					
137	543	514	557	526	552	530	*545*	522	545
53	556	540	570	554	568	555	*559*	546	559
14A	537	507	543	516	576	552	*560*	537	560
6	575	584	603	611	600	605	585	*591*	591
23	598	572	614	585	616	594	*605*	583	605
Avg.	562(25)	543(34)	577(30)	558(40)	582(26)	567(31)	571(24)	556(30)	572(25)†
				Grade 6 (M_3)					
79††	487	494	506	514	538	542	526	*532*	532
4A	541	553	574	582	586	586	566	*568*	568
47	575	548	596	568	595	572	*578*	556	578
19	575	551	585	562	606	579	*589*	566	589
112	576	530	589	538	614	577	*595*	557	595
50	595	578	606	586	619	599	*607*	589	607
63	587	557	606	576	626	600	*610*	585	610
30	595	559	615	578	639	606	*616*	584	616
8	631	611	654	635	646	625	*628*	609	628
140	625	588	637	600	652	615	*632*	598	632
Avg.	589(27)	564(24)	607(25)	581(27)	620(23)	595(18)	602(22)	579(18)	603(22)
				Grade 6.5 (M_5)					
77-3	624	598	635	609	634	611	*619*	597	619
77-2	636	606	647	617	646	620	*630*	605	630
90	632	623	640	631	657	645	*637*	626	637
76	636	605	647	616	660	630	*641*	613	641
56	636	593	652	609	657	620	*641*	606	641
91	656	627	666	637	689	661	*669*	643	669
Avg.	637(11)	609(14)	648(11)	620(12)	657(18)	631(19)	640(17)	615(17)	640(17)
				Grade 7 (M_5)					
73	630	601	643	614	660	637	*640*	616	640
87	665	629	690	654	666	640	*657*	631	657
143	675	621	686	633	668	631	*658*	620	658
145	666	666	675	675	674	674	*663*	663	663
96	712	656	718	662	682	644	*675*	636	675
Avg.	670(29)	635(29)	682(27)	648(24)	670(8)	645(17)	659(13)	633(19)	659(13)‡
				Grade 8 (M_5)					
11	779	716	805	741	726	682	*719*	675	719‡‡
Avg.§	25.8	23.8	25.2	24.8	20.7	21.8	21.7	22.0	
Avg.§§	22.5		23.2		20.3		20.8		

Note: References: Ferry and Spear (1978); Hodges and Spear (1982); Ganguly and Saxena (1984, 1985). A nominal *P* of 3500 bars was assumed. "A" with sample number indicates presence of M_2 andalusite. Values in parentheses are one standard deviation.

* Ganguly and Saxena with ΔW_{Mn} reduced from 3000 ± 500 to 2500 cal. Peak *T* italicized and given in last column.

** These three specimens are probably M_2.

† Inclusion of three specimens studied by Dutrow (1985) (237, 580 °C; 330, 592 °C; 267, 613 °C) increases this value to 581(24) °C, presumably a more accurate value because *T* of specimen 137 might be retrograde.

†† Specimen has textural indications of retrogression; excluded from all averages and from geobarometry.

‡ This value may be reduced by a maximum of 7 °C to compensate for change in biotite composition during early cooling (see text).

‡‡ May be reduced by a maximum of 20 °C (see text).

§ Weighted average of standard deviations, grades 4–7.

§§ Weighted average of peak temperature standard deviations, grades 4–7.

Most calibrations after 1978 use Ferry-Spear K_D data and empirically correct for nonideality, principally from Ca and Mn in garnet. A nominal pressure of 3.5 kbar was used for the calculations.

The quality of these calibrations as they relate to the Maine rocks may be evaluated by comparing the temperatures with temperature estimates based on dehydration equilibria (discussed below) and by comparing the scatter of the data and the overlap between grades. Comparison of the calibrations centers mainly on grades 5 and 7. Each of these zones may represent a relatively narrow T range (assuming a limited range of X_{H_2O}) because each involves a univariant reaction in the model KFMASH system. For grade 5 (staurolite breakdown), the modified Ganguly-Saxena calibration involves the smallest standard deviation, and the Hodges-Spear involves the largest (see also Dutrow, 1985). For grade 7 (muscovite breakdown), the original Ganguly-Saxena calibration appears best, and the Ferry-Spear appears worst. If all the standard deviations of grades 4–7 are averaged, the original Ganguly-Saxena is slightly lower than the modified Ganguly-Saxena (Table 8). This may be due to the fact that the Ganguly-Saxena corrections are partly based on best-fit calculations of data similar to ours.

A partial test of the accuracy of the geothermometric methods is provided by the two garnet-zone specimens. Stability considerations for staurolite-almandine (e.g., Ganguly, 1969) and fluid-composition considerations (e.g., Holdaway, 1978) suggest that in graphite-bearing rocks the staurolite isograd should occur at about 520 °C at 3–4-kbar pressure. The garnet-zone specimens come from field positions very near the staurolite isograd (chloritoid does not occur in M_3). The high Mn content (up to 28 mol%) of garnet-zone garnets causes the various calibrations to spread out over a wide T range. The modified Ganguly-Saxena calibration appears to provide the best temperatures for this zone, while the original Ganguly-Saxena provides slightly higher temperatures that overlap with several of the staurolite-zone temperatures. It appears that the Ganguly-Saxena calibration with $\Delta W_{Mn} =$ 3000 cal slightly overcompensates for nonideality of spessartine component.

Temperatures that estimate peak metamorphic conditions are listed in the last column of Table 8. In grades 3 and 4, much of the zoning is of a prograde nature, whereas in grades 5 through 8, diffusion zoning and retrograde growth zoning are prominent as indicated by intermediate-zone temperatures that are lower than core temperatures.[4] In grades 5 through 8, the intermediate-zone temperatures are more accurate than the core temperatures because the adjacent biotite was equilibrated with intermediate-zone compositions last. However, temperature estimates record an event during the cooling cycle at which diffusion between garnet and biotite was frozen in.

[4] Note that although final biotite composition was used for core and intermediate-zone garnet-biotite temperatures, the T effect on biotite composition is quantitatively unimportant as shown in footnote 2.

Once K-feldspar had formed in grades 7 and 8, garnet may have reacted with K-feldspar during retrograde metamorphism (Fig. 3) to make biotite more Fe-rich than that at equilibrium with the garnet cores. Thus the garnet core temperatures in grades 7 and 8 may be higher than equilibrium values, whereas the intermediate-zone temperatures are more accurate but are retrograde in nature. An estimate of the maximum extent of this effect may be made by comparing the average difference between core and intermediate-zone temperatures for grades 6.5 and 7. In grade 6.5, ΔT is 25 °C, and in grade 7 it is 32 °C (if the unzoned specimen 145 is excluded). Thus, the grade 7 rocks from the same region as grade 6.5 rocks have a maximum T effect of about 7 °C because of the change in biotite composition. For the single grade 8 specimen, the maximum effect is 20 °C.

Peak temperatures from grade 5 (staurolite breakdown) average 572 ± 25 °C. However, the temperature for specimen 137 (545 °C) may be retrograde. Addition of three specimens from the Farmington quadrangle [Dutrow, 1985; Table 8, grade 5 (M_3) average] increases the average to 581 ± 24 °C, which may be a better average for grade 5.

Approximate temperatures are grade 3, <510; grade 4, 510–560; grade 5, 560–595; grade 6, 595–625; grade 6.5, 625–645; grade 7, 645–670; grade 8, >670 °C (Table 8). The largest deviation of any specimen from these ranges is 25 °C which is an approximate indication of (2σ) precision. This is in rough agreement with analyses of two different garnet grains in each of three samples (5, 19, and 56) that average a 19 °C difference and with analyses of two specimens from 4 m apart in the same outcrop (77-3, 77-2, Table 8) that differ by 11 °C. A further test of the accuracy of these temperatures is given in a subsequent section. It is important to note that grades 6 and 6.5, which have the same mineral assemblages, show almost no overlap in calculated temperatures. In our opinion, this is because they crystallized during different events at different pressures as discussed below.

Geobarometry

Three geobarometers have possible value in medium- to high-grade pelitic metamorphic rocks: the phengite geobarometer (e.g., Powell and Evans, 1983); the garnet–aluminum silicate–plagioclase (GASP) geobarometer, most recently calibrated by Newton and Haselton (1981) and improved by the garnet mixing models of Ganguly and Saxena (1984); and the muscovite-almandine-biotite-sillimanite geobarometer (MABS) approximately calibrated by Spear and Selverstone (1983) and Robinson (1983). There are presently large uncertainties in the phengite geobarometer, especially for low-pressure rocks where the phengite content of muscovite is small and highly dependent on the method of calculating end members and activity models (see mineral-chemistry section). Also the method requires the presence of primary chlorite, and many of these rocks contain only chlorite interpreted to be retrograde. The GASP geobarometer suffers from the low grossular contents of garnets and variable

zoning of plagioclase compositions in these low-pressure rocks. Although in need of further calibration and testing, the MABS geobarometer may become the best barometer for pelitic rocks because all the components involved in the reaction are major components in the minerals.

Pressure of zone 5. The first appearance of sillimanite in M_3 is by reaction of staurolite with quartz in grade 5. Garnet-biotite temperatures for this zone indicate that sillimanite began to form at ~560 °C (Table 8). M_3 is defined as metamorphism in which the aluminum silicate produced as a staurolite breakdown product was sillimanite. The aluminum silicate diagram of Holdaway (1971) shows that this must have occurred at a pressure above ~3.0 kbar. Because M_3 immediately followed M_2, and locally the transition from M_2 to M_3 is nearly continuous (Novak and Holdaway, 1981), it is reasonable to assume that average M_3 pressure was only slightly above this value. There is also an andalusite locality near Farmington (Dutrow, 1985) that cannot be explained as earlier M_2, but may well represent a slight northward P decrease during M_3. If the average M_3 pressure was 3.5 kbar, as determined by Ferry (1976) and generally accepted by other workers in the area, garnet-biotite temperatures show that some relict M_2 andalusites would have occurred in the sillimanite P-T field, without nucleation of sillimanite. For the purpose of calibrating the MABS geobarometer we have assumed an average P for M_3 of 3.1 ± 0.25 kbar. Although the 3.1-kbar P estimate is adopted as the average pressure for grades 5 and 6 and is reasonable for grades 3 and 4 (which show close spatial association with grades 5 and 6), one cannot assume that pressure remained constant in grades 6.5 through 8. These zones are exposed considerably south of most M_3 rocks and suffered later M_5 effects (Fig. 1).

MABS geobarometry. For grades 5 and 6, the present analyses and those of Dutrow (1985) in the southern 40% of the Farmington quadrangle provide a unique opportunity to calibrate the geobarometer involving the assemblage muscovite-almandine-biotite-sillimanite (Fig. 3) that occurs in all rocks from grades 5 to 8. The ideal end-member reaction is

$$\underset{\text{Muscovite}}{KAl_2AlSi_3O_{10}(OH)_2} + \underset{\text{Almandine}}{Fe_3Al_2Si_3O_{12}} = \underset{\text{Annite}}{KFe_3AlSi_3O_{10}(OH)_2} + \underset{\text{Sillimanite}}{2Al_2SiO_5} + \underset{\text{Quartz}}{SiO_2}. \quad (3)$$

All analyzed M_3 specimens from grades 5 and 6 were used with the exception of one retrograded specimen each from the present analyses and from the Dutrow (1985) analyses. All specimens were assumed to have crystallized at an average P of 3.1 kbar and peak temperature as defined by the modified Ganguly and Saxena (1984, 1985) garnet-biotite geothermometer (Table 8).

The equilibrium constant K^* was evaluated using the following activity models to adjust actual mineral compositions to ideal end-member compositions: $a_{Alm} = (X_{Fe}^{Grt})^3(\gamma_{Fe}^{Grt})^3$; $a_{Ms} = (X_{Al}^{Ms})^2 X_{\square}^{Ms} X_K^{Ms} \gamma_K^{Ms}$; $a_{Ann} = (X_{Fe}^{Bt})^3 X_K^{Bt}$; $a_{Sil} = 1$; $a_{Qtz} = 1$. Fe was assumed to be disordered on the M(1) and M(2) octahedral sites of biotite. Activity coefficients were calculated for almandine component following Ganguly and Saxena (1984) with $\Delta W_{Mn} = 2500$ cal. The value of $(\gamma_{Fe}^{Grt})^3$ varies from 0.90 to 1.11. Activity coefficients for K in muscovite were evaluated assuming that pyrophyllite component behaved like muscovite component and γ_K^{Ms} was based on paragonite component only. The equation of Chatterjee and Flux (1986) for muscovite was used. Biotite was assumed to be ideal. This is partly because of the absence of data and partly because the amounts of most of the other components were small enough to have negligible effects on the major components. The possible nonideality of Al in biotites tends to cancel out because the calibration was done on Al-rich biotites. Tetrahedral sites were assumed to be coupled to octahedral or 12-fold sites.

The value of ΔP corrected for observed mineral compositions is given by

$$\Delta P = -\Delta V^{-1} RT \ln K^*, \quad (4)$$

where ΔV is given in Table 9. A plot of ΔP against T was used to determine the end-member P-T curve for Reaction 3. The resulting equation is

$$P = 15(T - 968) + \Delta P, \quad (5)$$

where P is in bars and T is in kelvins.

Calculated pressures for the rocks from grades 5 and 6 (M_3) from Dutrow (1985) and the present study are shown in Figure 6, whereas all calculated pressures from the present study are given in Table 10. The approximate constancy of pressure for grades 5 and 6 indicates that the slope of about 15 bars/K is reasonable. Attempts were made to calculate the slope from entropy and volume data (Table 9). For Reaction 3, ΔS varies between −6.8 and +5.6 J/K depending on the choice of entropy for almandine and sillimanite. This would allow a maximum slope of +3.6 bars/K for the reaction, suggesting that the thermodynamic data are less precise than the present calibration. If we assume that the best values for sillimanite and almandine entropy are those of Robie and Hemingway (1984) and Chatillon-Colinet et al. (1983), respectively, and that the muscovite entropy is accurate, then the annite entropy would need to be about 29 J/K higher than the value given by Helgeson et al. (1978) in order to be consistent with the 15 bars/K slope.

Several arguments suggest that much of the scatter in Figure 6 (3.09 ± 0.38 kbar) results from analytical error, temperature error, and imperfect equilibration rather than real variation in P: (1) For grades 5 and 6, the Dutrow (1985) specimens show as much scatter in P as the specimens from this report collected over a much wider area. (2) The distribution of P values for M_3 is nearly random on the map as shown in Figure 1. Considering these observations and the smaller spread of P values for grade 6.5 (±0.19), we estimate the (2σ) error for the method at 0.5 kbar.

Specimens from grade 6.5 (M_5) indicate consistent pres-

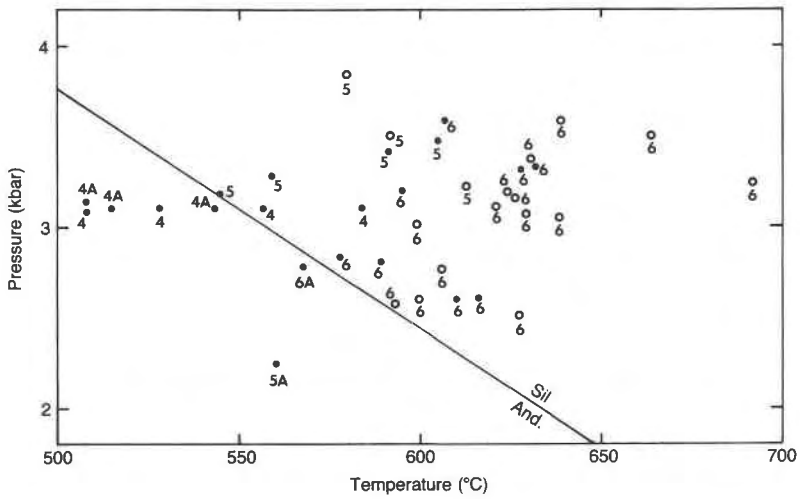

Fig. 6. *P-T* plot for M_3 metamorphic grades 4, 5, and 6 using present data (dots) and those of Dutrow (1985) for southern Farmington quadrangle (circles). "A" indicates M_2 andalusite present. Temperature is that of the modified Ganguly-Saxena (1984) garnet-biotite geothermometer (Table 8), and pressure is based on the MABS geobarometer (Table 10). Sillimanite-absent rocks are plotted at 3.1 kbar, the average *P* for M_3 (see text). Only two specimens (a 6A and a 5A containing M_2 andalusite and M_3 sillimanite) plot incorrectly in the andalusite field. Much of the scatter from the average 3.1 kbar represents analytical error, temperature error, and incomplete equilibration. Temperature error (2σ) is ± 25 °C.

sures of 3.81 ± 0.19 kbar (Table 10, Figs. 1, 7), or about 700 bars above the prevailing *P* during M_3. This is consistent with the recent discovery of kyanite in M_5, 35 km southwest of Lewiston (Fig. 1) on the south side of the Sebago batholith (Thomson and Guidotti, 1986; Hussey et al., 1986). For grades 7 and 8, from the same M_5 area as grade 6.5, pressures from all but the lowest-*T* specimen of grade 7 are higher and rather variable (Table 10, in brackets). Possibly, the presence of K-feldspar, implying partial reaction of biotite and sillimanite to garnet, K-feldspar, and fluid (Fig. 3), disturbs the equilibration of garnet and muscovite with biotite and sillimanite. Consequently, the geobarometer should be used with caution in K-feldspar–bearing rocks. An alternative explanation is that the M_5 rocks share a complicated metamorphic history, and the grade 6.5 rocks have most completely equilibrated to a single (presumably the latest) metamorphic event.

Dehydration equilibria

Univariant dehydration reactions in the model KFMASH system involving breakdown of staurolite and muscovite were applied to grades 5 and 7, respectively. Two alternative approaches are (1) to assume that the determined *P* and *T* values are correct and solve for X_{H_2O} in the fluid, or (2) to assume values for X_{H_2O} consistent with presence of graphite in reducing rocks and test for consistency between *P*, *T*, and X_{H_2O}. In our opinion, X_{H_2O} in graphitic pelites is better constrained than *P* or *T*, and thus we have chosen the second approach.

H_2O content of fluid. As shown by Ohmoto and Kerrick (1977), the mole fraction of H_2O in the fluid of graphite-bearing rocks is a slowly varying function of *P* and *T* and a rapidly varying function of the relative amounts of CO_2 and CH_4 in the fluid (or, alternatively, of the f_{O_2}). We have calculated values of a_{H_2O} at the equil-

TABLE 9. ΔS and ΔV for Reactions 3, 7, and 8

Reaction	*T* (°C)	*P* (kbar)	ΔS_r (J/K)	ΔV_r (J/bar)	References, notes*
(3) Alm + Mus	610	—	−6.84	2.082	a, b, d
	610	—	−3.32		a, b
	610	—	2.11		a, c, d
	610	—	5.63		a, c
(7) Mus + Qtz	660	3.8	75.77		a, f, i
(8) St + Qtz	660	4.125	122.49	3.550	a, b, d, e, f, g, h
	660	4.125	109.09		a, c, d, f, g, h
	610	3.1	128.64		a, b, d, f, g, h

* a = Helgeson et al. (1978) (*S*, *V*, and C_p), except as noted. b = Metz et al. (1983) (Alm *S*); Helgeson et al. (1978) (Alm C_p). c = Chatillon-Colinet et al. (1983) (Alm *S*); Helgeson et al. (1978) (Alm C_p). d = Robie and Hemingway (1984) (Sil *S*, C_p). e = Richardson (1966) (St *V*). f = Burnham et al. (1969) (H_2O *V*, *S*). g = Hemingway and Robie (1984) (St *S*, C_p). h = See appendix for calculation of chemical and disorder effect on staurolite. Staurolite formula given in Reaction 8. i = Helgeson et al. (1978) data used for internal consistency.

TABLE 10. Pressure determinations based on the almandine-muscovite geobarometer

No.	T* (°C)	P (kbar)	No.	T* (°C)	P** (kbar)
	Grade 5 (M_3)			Grade 6.5 (M_5)	
137	545	3.18	77-3	619	4.03
53	559	3.28	77-2	630	3.96
14A	560	2.24	90	637	3.52
6	591	3.41	76	641	3.77
23	605	3.37	56	641	3.67
Avg.	572(25)	3.12(50)	91	669	3.90
			Avg.	640(17)	3.81(19)
	Grade 6 (M_3)				
4A	568	2.77		Grade 7 (M_5)	
47	578	2.83	73	640	3.80
19	589	2.80	87	657	[4.71]
112	595	3.19	143	658	[5.08]
50	607	3.59	145	663	[5.13]
63	610	2.60	86	675	[5.93]
30	616	2.60	Avg.	659(13)	[4.93(77)]
8	628	3.31			
140	632	3.33		Grade 8 (M_5)	
Avg.	603(22)	3.00(36)	11	699	[6.24]

* Peak garnet-biotite T (Table 8).
** Brackets indicate uncertain values (see text).

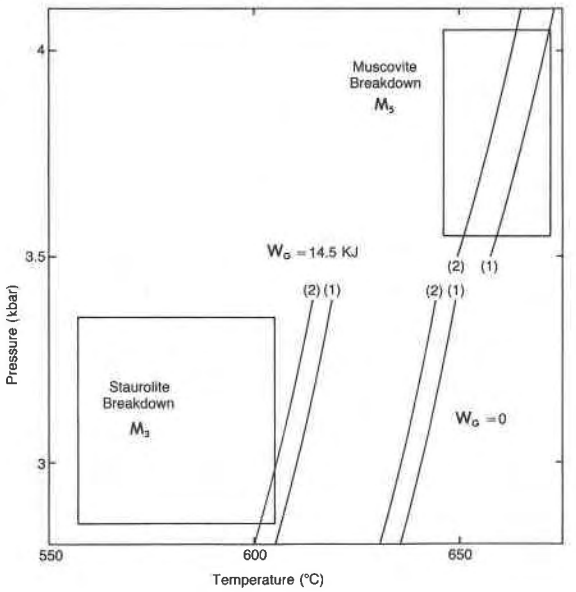

Fig. 7. Comparison of average T determined by garnet-biotite geothermometry (boxes) and average T determined from dehydration equilibria (curves) for Reactions 7 and 8 in grades 7 (M_5) and 5 (M_3), respectively. Numbers in parentheses indicate models for reaction of water with graphite discussed in the text. For grade 5, two possibilities are indicated: W_G = 0 kJ per staurolite tetrahedral site and W_G = 14.5 kJ per site as discussed in text. Data from Tables 12 and 13.

ibration T (calculated from garnet-biotite equilibrium) for Reactions 7 and 8 for P-T conditions of grades 5 and 7 on the basis of two models: (1) The pelitic rocks acted as closed systems, and graphite reacted with H_2O of dehydration to produce equimolar amounts of CO_2 and CH_4:

$$2C + 2H_2O = CO_2 + CH_4. \quad (6)$$

(2) CO_2, being several times the size of CH_4, escaped from the rocks more slowly and/or was added to the pelites from the rare metacarbonate rocks of the area. Metacarbonate rocks equivalent to grades 5 and 6 at the eastern edge of the present area contained fluids with $X_{H_2O} \geq 0.78$ (Ferry, 1980). We assume a limiting case of $X_{CO_2} = 10X_{CH_4}$. The majority of graphite-bearing pelites with low f_{O_2} should have X_{H_2O} values between these extremes. The sources of data and results of these calculations are summarized in Table 11. Other fluid species (H_2, H_2S, CO, etc.) are assumed to be quantitatively unimportant (Ohmoto and Kerrick, 1977).

Muscovite-quartz reaction. In grade 7, the model univariant reaction

$$\underset{\text{Muscovite}}{KAl_3Si_3O_{10}(OH)_2} + \underset{\text{Quartz}}{SiO_2} = \underset{\text{K-feldspar}}{KAlSi_3O_8} + \underset{\text{Sillimanite}}{Al_2SiO_5} + \underset{\text{Fluid}}{H_2O} \quad (7)$$

was in progress over a relatively narrow T range in all the rocks. Using the activity model discussed above for muscovite, X_K^{Kfs} for K-feldspar, and activity coefficients calculated from Chatterjee and Flux (1986) for muscovite and Waldbaum and Thompson (1969) for K-feldspar, the T separation between the experimental curve and natural occurrences was calculated. The relationship is

$$\Delta T = RT_f \ln(K^* a_{H_2O}^n) \Delta S_r^{-1}, \quad (2)$$

where K^* is the equilibrium constant based on solid solution of muscovite and K-feldspar, ΔS_r is given in Table 9, and n is the number of moles of water in the reaction (Kerrick, 1974). At 3.8 kbar, the pressure assumed for all M_5 in the area (Table 10), the pure phases of Reaction 7 are stable at 664 °C (Chatterjee and Johannes, 1974). Final results of calculations are given in Table 12 and illustrated in Figure 7.

The agreement between garnet-biotite and muscovite-quartz temperatures is excellent. The accuracy of calibration of each geothermometer is estimated to be ±15 °C,

TABLE 11. Mole fractions for water in graphite-bearing pelites

T (°C)	P (kbar)	Model 1 a_{H_2O}	Model 2 a_{H_2O}
660	3.8	0.903	0.831
620	3.1	0.902	0.831
580	3.1	0.919	0.860

Note: Calculated using data of Ohmoto and Kerrick (1977) for thermodynamic data of Reaction 6, Burnham and Wall (unpub. data) for CO_2 fugacity coefficients, Burnham et al. (1969) for H_2O fugacity coefficients, Ryzhenko and Volkov (1971) for CH_4 fugacity coefficients, and Kerrick and Jacobs (1981) for H_2O-CO_2 mixing relations. Because of its nonpolar nature and similar fugacity coefficient to CO_2, CH_4 was assumed to mix with the same mixing activity coefficient as CO_2.

TABLE 12. Temperatures (°C) of grade 7 (M_5) based on muscovite-quartz reaction and presence of graphite at 3.8 kbar

No.	K^*	$T_{G\text{-}B}$**	T—Model 1†	T—Model 2†
73	1.143	640	667	659
87	1.166	657	669	661
143	1.108	658	664	656
145	1.125	663	666	657
86	1.178	675	670	662
Avg.	1.14(3)	659(13)	667(2)	659(3)

* K^* includes activity coefficients for muscovite and K-feldspar.
** Peak garnet-biotite T (Table 8).
† See text and Table 11. Calculated using Equation 2, initial T of 664 °C (Chatterjee and Johannes, 1974), and ΔS_r = 75.77 J/K (Table 9).

suggesting that the averages of the two methods should agree within about 21 °C ($\sqrt{15^2 + 15^2}$). Model 1 ($X_{CO_2} = X_{CH_4}$) yields T 8 °C higher and model 2 ($X_{CO_2} = 10X_{CH_4}$) yields T equal to the average garnet-biotite temperature for grade 7. The maximum separation between a garnet-biotite and the corresponding muscovite dehydration T based on precision alone (95% confidence level) should be less than $2\sqrt{13^2 + 3^2}$ or 27 °C. For model 1 the maximum difference between the methods is 27 °C, and for model 2 this maximum is 19 °C (Table 12). This analysis suggests that (1) much of the scatter in garnet-biotite temperatures for grade 7 is due to precision error and does not represent real variation in T and (2) model 2 *may* be slightly better than model 1 for muscovite breakdown, although real variation in X_{H_2O} is probable. There is nothing in the results to suggest lower values of X_{H_2O} than those of model 2 (0.78). Inspection of the values of K^* and T from model 2 (Table 12) shows that the effects of small amounts of octahedral Fe, Mg, and Ti in muscovite[5] roughly cancel out the effects of CO_2 and CH_4 in the fluid and greater Na in K-feldspar than in muscovite.

The excellent agreement between the muscovite dehydration equilibrium and garnet-biotite temperatures gives credence to the average values of garnet-biotite temperatures and to the two models for the behavior of H_2O in reduced graphitic systems. In addition, the preservation of graphite and reduced nature of the ilmenite indicate that large volumes of pure H_2O have not moved through these rocks and that reasonable amounts of CH_4 remained in the equilibrium fluid.

[5] Various workers (e.g., Speer, 1984, p. 329) have implied that the data of Velde (1965) require that celadonite component must reduce the thermal stability of muscovite. The *initial* effect of celadonite component must relate to Reaction 7. Because Al in muscovite is diluted much more than Al in sillimanite and K-feldspar, muscovite stability must first be increased, reach a maximum, and then be decreased according a reaction such as celadonite $_{ss}$ + sillimanite = muscovite + biotite. The reaction studied by Velde is not directly applicable to most pelitic rocks because it involves K-rich bulk compositions producing K-feldspar in the absence of aluminum silicate. Velde's study does demonstrate that muscovite-celadonite solid solution cannot be far from ideal.

Staurolite-quartz reaction. In grade 5 all specimens contain an assemblage relating to the FASH model reaction

$$\underset{\text{Staurolite}}{H_3Fe_{4.3}Al_{17.92}Si_{7.66}O_{48}} + 4.166\underset{\text{Quartz}}{SiO_2} = 7.527\underset{\text{Sillimanite}}{Al_2SiO_5} + 1.433\underset{\text{Almandine}}{Fe_3Al_2Si_3O_{12}} + 1.5\underset{\text{Fluid}}{H_2O}. \quad (8)$$

The staurolite formula used above is an Fe end-member formula for graphite-bearing rocks based on the chemical study of Holdaway et al. (1986b). The H content is consistent with analyzed H values from the present study (Table 4). As shown in Appendix 1, an activity model for staurolite can be formulated using the results of Holdaway et al. (1986b).

Fe end-member staurolite breaks down along a stability curve bracketed by temperatures of 645 and 660 °C at 3.25 kbar and 675 and 690 °C (but very close to 690 °C) at 5 kbar (Dutrow and Holdaway, 1983; Dutrow, 1985; Dutrow and Holdaway, in prep.). This stability curve for Reaction 8 results from a careful SEM study of reaction products and is consistent with the earlier experiments of Richardson (1968) at moderate pressures. Calculated ΔS values for Reaction 8 (Table 9) were compared with slope calculations based on the experimental results. The experiments indicate an average slope between 39 and 117 bars/K, whereas the Metz et al. (1983) almandine entropy indicates a slope of 34.5 bars/K, and the Chatillon-Colinet et al. (1983) almandine entropy indicates a slope of 30.7 bars/K (Table 9). The agreement is good considering the magnitude of errors both in ΔS and in the experimental slope. A value of 128.64 J/K was chosen for the approximate midpoint between the experimental and natural T conditions, consistent with the Metz et al. (1983) almandine entropy. The slope data are not precise enough to select between the Metz et al. (1983) and Chatillon-Colinet et al. (1983) almandine entropies, but they do suggest that both entropies are reasonable.

Using Equation 2, the almandine activity model discussed previously, the staurolite activity model given in Appendix 1, and the fugacity ratios of Table 11, values of T were calculated and are tabulated in Table 13 for both models of fluid behavior. An initial T of 645 °C was chosen for the experimental end-member reaction at 3.1 kbar, consistent with the experiments and with the calculated slope values. Despite the improvement in ΔS, staurolite stability relations, staurolite formula, and garnet-biotite geothermometry, there remains a 57–62 °C discrepancy between average T calculated from garnet-biotite geothermometry and that determined from staurolite stability relations (Fig. 7). Such discrepancies have also been noted by many other workers (e.g., Pigage and Greenwood, 1982; McLellan, 1985). Previously, we believed that these discrepancies resulted mainly from problems in the crystal chemistry and stability relations of staurolite (Holdaway et al., 1986b). However, it now becomes clear that there must be additional causes, the most likely being nonideality in staurolite tetrahedral sites.

Nonideality in staurolite solid solution is further evidenced by values of K^* for Reaction 8 (Table 13). Since the staurolites all crystallized over a limited T range, K^* should be roughly constant, as it is for muscovite (Table 12). Instead K^* is high for staurolites low in Fe and low for staurolites high in Fe. The K^* values indicate that, for three specimens, solid solution reduces equilibrium T and, for the other five, solid solution increases T, if water dilution is ignored. The temperatures calculated for the

most Fe-rich staurolite (specimen 53) most closely approximate the average garnet-biotite temperature, whereas those for the most Mg-rich staurolites are farther from the average garnet-biotite temperature (Table 13), again suggesting nonideality. Recent high-P experimental studies of Rice (1985) can only be explained by nonideal solid solution.

If we exclude specimen 6, a high-Li staurolite, all the staurolites of this study contain at least 3.01 Fe atoms. The great majority of staurolites are Fe-rich, and those with high Mg appear to be high-P, high-T staurolites (e.g., Schreyer et al., 1984). Holdaway et al. (1986b) provide strong evidence, based on high-quality complete chemical analyses, that Fe, Mg, Zn, and Li may be assigned to the tetrahedral Fe sites. Using this assumption, we postulate a regular-solution (pseudobinary) model for staurolite with tetrahedral ions grouped in two categories: Fe and vacancies as one, and Mg, Zn, and Li as the other. The justifications for this are (1) vacancy content of tetrahedral sites may vary substantially with presence or absence of coexisting R^{2+} phases and (2) ionic radii and maximum solid solution of Mg, Zn, and Li are comparable (e.g., Holdaway et al., 1986b). The approach can only be expected to work well for an (Fe,Mg)-dominated staurolite with minor Li, Zn, and vacancies. A Margules parameter of 15 kJ per tetrahedral site produces a solvus that passes through T-X_{Fe} values for five of the staurolite analyses, leaves all the remaining analyses outside of the solvus, and has a crest at 600 °C. From this maximum possible W_G value, activity coefficients were calculated. The activity model for the present situation becomes ${}^{iv}\gamma^{4}_{Fe} \times {}^{iv}X^{3.9}_{Fe} \times {}^{U}X^{0.25}_{Fe}$.

The results (Table 13) show that the use of 15 kJ for W_G overcorrects the Li-rich specimen, suggesting that the Fe-Li interaction has a W_G lower than 15 kJ. For the other staurolites, a tighter spread in T results. For model 1, the T averages 32 °C above that indicated by garnet-biotite geothermometry, whereas model 2 indicates an average T that is 27 °C above the garnet-biotite average (Fig. 7). Specimens with large differences in Fe content but similar Li contents (e.g., 53 and 14) show similar calculated temperatures. The 27–32 °C difference in average T is very reasonable in light of the various errors involved in garnet-biotite geothermometry, in the oversimplified staurolite solution model, in estimating W_G, and in the fluid-composition models.

The behavior of staurolite may be somewhat analogous to that of the muscovite-paragonite system. A (metastable) breakdown curve for the Mg staurolite end member in equilibrium with muscovite and quartz probably occurs at lower temperatures than that for the Fe staurolite end member. Even though the Mg end member is unstable at low pressures, the Fe limb of the Fe-Mg solvus still approximately controls the limiting composition of Fe-rich staurolite in the same way that the muscovite-paragonite solvus controls the limiting composition of muscovite even at conditions where paragonite is unstable. Analogous to paragonite, Mg staurolite is stable at high pressures (Schreyer and Seifert, 1969). This model may be tested by seeking (experimentally and in the field) coexisting Fe- and Mg-rich staurolites at high P and T that equilibrated below 600 °C.

It is important to distinguish between what can be said regarding staurolite nonideality with reasonable certainty and what remains as conjecture. (1) We can be reasonably certain that staurolite behaves nonideally. The present model distributes the diluting ions Mg, Zn, and Li over about four sites. No ideal model can be used to account for the ~50 °C difference between garnet-biotite T and T based on Reaction 8, when one considers that Fe-Mg K_D values between staurolite and garnet are close to unity and Zn and Li in staurolite approximately compensate for Mn in garnet (note K^* values averaging 1.10 in Table 13). The only way K^* could be reduced slightly would be if the diluting ions in staurolite were distributed over less than four sites (presumably 2). This is very unlikely because Mg-rich staurolites contain more than 2 (Mg + Zn) (Schreyer et al., 1984), and synthetic Mg staurolite contains substantially more than 2 Mg (Schreyer and Seifert, 1969). (2) The assignment of Fe, Mg, Zn, and Li to tetrahedral sites is slightly less certain, although Holdaway et al. (1986b) have made a strong case for it. (3) Assuming nonideality in the tetrahedral Fe sites, approximations that require further testing and refinement are the pseudobinary model, the regular-solution assumption, and the exact value of W_G. The value of W_G chosen is the maximum possible one, and it still doesn't fully compensate for the T difference between garnet-biotite geothermometry and staurolite stability.

The suggestion of a Margules parameter of ~15 kJ per site for staurolite may provide an explanation for reversals that occur in Fe-Mg partitioning of staurolite vs. other minerals. Grambling (1983) has observed a reversal in staurolite-chloritoid partitioning caused by an increase in Mg. Chloritoid contains more Fe than staurolite in very Fe-rich compositions and more Mg than staurolite at more Mg-rich compositions. A comparable reversal may occur with staurolite-almandine at much more Mg-rich compositions than those observed here (Schreyer et al., 1984). The estimated W_G should be tested against these K_D reversals, which may well provide a very sensitive indicator.

TABLE 13. Temperatures (°C) of grade 5 (M_3)

			$W_G = 0$		$W_G = 15$ kJ/site	
No.	K^*	T_{G-B}	T (1)	T (2)	T (1)	T (2)
137	1.152	545	647	642	619	615
53	0.953	559	636	631	613	608
14	1.272	560	653	648	609	605
237**	1.095	580	644	639	618	613
6	1.246	591	652	643	[578]	[573]
330**	0.993	592	639	634	609	604
23	1.006	605	639	634	609	604
267**	1.110	613	646	640	612	608
Avg.	1.10(12)	581(24)	645(6)	639(6)	608(13)	604(13)
Avg.‡			643(6)	638(6)	613(4)	608(4)

Note: Temperatures based on staurolite-quartz reaction and presence of graphite at 3.1 kbar. Calculated using Equation 2 and initial T of 645 °C (Dutrow and Holdaway, in prep.). ΔS, for the calculations was 128.64 J/K (Table 9). T (1) = from model 1; T (2) = from model 2. Values given in brackets correspond to a Li-rich staurolite whose activity coefficient is overcorrected by the pseudobinary model discussed in the text.

* Equilibrium constant = K^*.

** Specimens 237, 330, and 267 are from the Farmington quadrangle (Dutrow, 1985). See also Table 8, grade 5 (M_3) average.

‡ Excluding specimen 6.

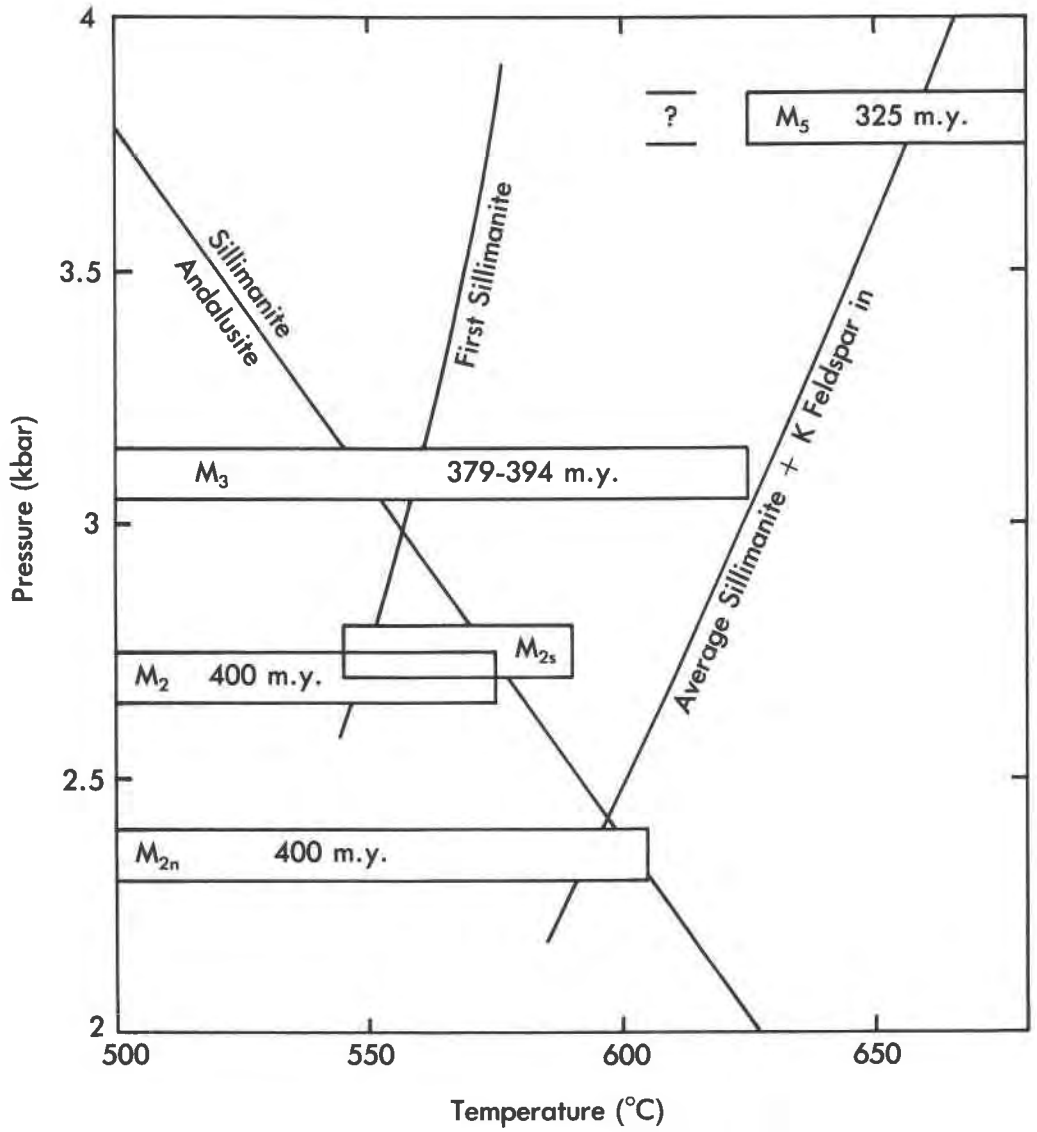

Fig. 8. Range of *P-T* conditions for various metamorphic events in west-central Maine. Approximate age of each event is given. Data are from Dickerson and Holdaway (ms.) and the present report. The sillimanite-andalusite boundary is from Holdaway (1971), the first sillimanite curve is the *beginning* of Reaction 8, and the average sillimanite–K-feldspar curve is the *average* appearance of this assemblage by Reaction 7.

The results of geothermometry, geobarometry, and dehydration geothermometry are consistent when staurolite nonideality is taken into account (Fig. 7). These results are in agreement with reasonable models for fluids (X_{H_2O} = 0.78–0.91) in reduced graphite-bearing rocks. In some previous studies, overestimation of pressure or the staurolite problem has led workers to suggest unrealistically low values of X_{H_2O}.

Causes of metamorphic conditions

The thermal events recognized as M_2, M_3, and M_5 provide a discontinuous record of pressure increase during a time interval between 400 and 325 Ma (Fig. 8). The locus of metamorphism moved southward during this time from Caratunk, 30 km north-northeast of Kingfield (Dickerson and Holdaway, ms.; Holdaway et al., 1986a), to the Norway-Lewiston region, a distance of about 125 km in a south-southwest direction. In discussing the causes of metamorphism, temperature and pressure will be treated separately. Although a detailed discussion of M_2 is not a topic of the present contribution, evidence from other sources will be used here to tie M_2 into the general picture of metamorphism for the region.

Temperature

With the exception of low-grade metamorphism M_1, all the metamorphic events in the area of Figure 1 show

a general spatial association with plutonic rocks (Fig. 1; Holdaway et al., 1986a). Many of the intrusive rocks of the area are sill-like bodies that pass gently beneath the surrounding metamorphic rocks, commonly with a northern dip (Hodge et al., 1982; Carnese, 1983). Modeling studies of Lux et al. (1986) and DeYoreo (1987) demonstrate that conditions such as those achieved at the culmination of M_2, M_3, and M_5 require the close proximity of magmatic heat. Even though isograds representing substantially increased T are commonly up to 10 km and rarely as much as 30 km from the exposed igneous rocks (Fig. 1; Holdaway et al., 1986a), the overall igneous spatial association and the gently dipping character of many of the igneous rocks imply that the batholithic heat sources lay no more than 1 to 3 km below the M_2, M_3, and M_5 isograds. This is shown by Lux and Guidotii (1985) and Guidotti et al. (1986) for the relation between the Sebago batholith and the M_5 sillimanite–K-feldspar isograd. In areas where isograds lie far from the igneous contacts and detailed geophysical studies fail to demonstrate that igneous rocks lie at depth, there is the possibility that gently dipping plutonic bodies once lay *above* the metamorphic rocks and acted as a heat source for metamorphism.

The conditions of grade 7, M_5 metamorphism (3.8 kbar, 660 °C) are very close to the invariant point at which the vapor-absent melting curve for muscovite-quartz-plagioclase occurs in graphitic pelites (Kerrick, 1972; Ohmoto and Kerrick, 1977). In this area (Fig. 1 in Holdaway et al., 1982) K-feldspar–absent rocks (6.5) are regionally interspersed with K-feldspar–bearing rocks (7) that clearly formed at a higher average T than grade 6.5 (Table 8). The large number of small granitic bodies and pegmatites suggests that incipient melting occurred in the rocks immediately below the present exposures, and varying degrees of upward transmission of magma and heat resulted. The incipient melting of these local magmas and the Sebago granites at slightly greater depth probably had a buffering effect on the rocks, preventing the total destruction of muscovite at the prevailing P, except in the single grade 8 specimen (11, Table 8) in which muscovite probably grew after the thermal culmination for the locality. In addition to T differences, minor differences in X_{H_2O} between grades 6.5 and 7 are possible.

Pressure

In west-central Maine, pressure increased from north to south and with time. The pressure of 2.35 kbar for the lowest-P portion of M_2 (Dickerson and Holdaway, ms.), average P of 3.1 kbar for M_3, and average P of 3.8 kbar for M_5 (Fig. 8) correspond to approximate depths of 8.2, 10.9, and 13.3 km, respectively, during the three events. M_2, M_3, and M_5 occurred at 400, 394–379, and 325 Ma, respectively, and at average distances of about 30, 80, and 110 km south-southwest of Caratunk where the lowest-P M_2 begins. This increase in P with map position and time may have been produced by two kinds of P increase: (1) an increase from north-northeast to south-southwest at any given time and (2) an increase with time at any given place. If one considers only the time, general spatial distribution, and P-T conditions of the three events, either of these two causes of P increase could have acted alone. Evidence cited below shows that both were necessary, perhaps each being responsible for about half of the pressure increase.

Change in P from north-northeast to south-southwest at a given time is difficult to document quantitatively, but a number of factors suggest that this has occurred: (1) The northern lobe of the Lexington batholith produced cordierite-andalusite (M_{2n}, $\sim 2.35 \pm 0.25$ kbar), whereas the central and southern lobes produced staurolite-andalusite (M_2, $\sim 2.7 \pm 0.25$ kbar; M_{2s}, $\sim 2.75 \pm 0.25$ kbar) (Dickerson and Holdaway, ms.; Holdaway et al. 1986a). The Gaudette and Boone (1985 and pers. comm.) age of 400 Ma is based on all three lobes, and none is distinguishable from the others beyond the limits of error. (2) Farther south, M_2 in the Kingfield and Anson quadrangles produces little or no garnet zone, and andalusite appears immediately after staurolite (Holdaway et al., 1986a). To the south near Farmington, the garnet zone widens to about 6 km, and andalusite first appears in the Dixfield quadrangle several kilometers west of the first M_2 staurolite (Dutrow, 1985). These observations are consistent with a southward P increase in M_2. (3) Dallmeyer (1979) has shown with incremental Ar-release ages on metamorphic biotites in an area along the eastern edge of Figure 1 (M_3 and M_5) that ages decrease *progressively* from about 330 Ma in the northeast to 230 Ma in the southwest. This slower cooling toward the southwest is consistent with a longer period of erosion to the biotite blocking isotherm or a higher initial T, hence the possibility of a deeper burial or slower uplift to the southwest. (4) In M_5 there must have been a P increase southwest across the Sebago batholith as indicated by P about 3.8 kbar on the north side compared with P of 5 kbar or more on the south side where kyanite routinely occurs with almandine-rich garnet (Thomson and Guidotti, 1986; Hussey et al., 1986; Carmichael, 1978). These observations require additional documentation, but a case for south-southwest increase in P appears to be emerging. This increase (perhaps equivalent to 2–3 km) probably represents a combination of slight tilting during post-metamorphic uplift and higher topography to the south-southwest during metamorphism.

The progressive increase in P with each subsequent event also requires changes in P with time as shown by the following evidence: (1) The transition from cordierite-andalusite (M_{2n}) to staurolite-andalusite (M_2, M_{2s}) occurs abruptly at the junction between the northern and central lobe of the Lexington batholith (Dickerson and Holdaway, ms.; Holdaway et al., 1986a), suggesting a rapid P increase over a small time interval near 400 Ma. This transition does not involve a fault, but does involve a change in igneous lithology. (2) In the Rangeley, Rumford, Phillips, Dixfield, Farmington, and Augusta quad-

rangles (Fig. 1), M_3 (no andalusite) is superimposed on M_2 (andalusite-bearing), indicating a P increase with time throughout these areas (Holdaway et al., 1982). (3) In the Bryant Pond, Buckfield, Livermore, and Lewiston quadrangles, there is a much less obvious superimposition of M_5 (~3.8 kbar) on M_3 (~3.1 kbar). In part this is less obvious because of the absence of a P-sensitive phase transition like andalusite-sillimanite. However, the appearance of retrogressive chlorite in the M_3 staurolite-grade rocks may be due to this effect.

The progressive increase in P with time requires the addition of perhaps 2–3 km of rock above the present level of exposure over a 75-m.y. period at a rate more rapid than erosion. This increase in overburden could have occurred over the whole region or could have been added in larger amounts in the southern and central parts of the area shown in Figure 1 than in the northern parts. The rock may well have been added both at the surface and at shallow crustal levels. There are several possible mechanisms whereby P may have increased with time: (1) Marine sedimentary and/or volcanic deposition could have continued throughout much of the time in question. This would have resulted from continued subsidence while plutonic rocks were being emplaced in great volume. However, the likelihood of surface subsidence during such a time is not great. (2) Nonmarine deposition could have been extensive with the build-up of a widespread volcanic highland. The P increase could have been accomplished by subsidence at the present level combined with intrusion at shallower levels and extrusion at the surface (see also Holdaway et al., 1982). The shallower igneous rocks would have been correlatives of the batholiths exposed at present levels. (3) A final possibility is emplacement of crust by overthrusting, presumably from the east. This model has problems because of the general absence of evidence of Middle Devonian to Mississippian thrusting. We prefer the model of emplacement of magmatic rocks at the surface and at levels shallower than present exposures. It should also be pointed out that the youngest rocks in west-central Maine are the Middle Devonian Tomhegan Formation, which is exposed 30 km north of the Lexington batholith and contains felsic tuffs, tuffaceous sedimentary rocks, and garnet rhyolite (Rankin, 1968). It is tempting to speculate that these are the earliest remnants of a more widespread volcanic terrane.

Conclusions

1. In west-central Maine, M_3 (394–379 Ma) includes the biotite, garnet, staurolite, staurolite-sillimanite, and sillimanite zones. The younger M_5 (325 Ma) includes sillimanite and sillimanite–K-feldspar within the second sillimanite isograd.

2. In these graphite-bearing pelitic rocks, the micas are well expressed in terms of conventional end members and "Ti-biotite" ($KTi\square(Fe,Mg)AlSi_3O_{10}(OH)_2$) or "Ti-muscovite" ($KTi(Fe,Mg)AlSi_3O_{10}(OH)_2$). Celadonite content of muscovite is very low and has a potentially large error. In determining mica end members, no substitution involving a combination of octahedral and 12-fold sites is required.

3. In garnet, the progressive changes in Mn content with T may be used to confirm previously suggested phase relations between garnet, staurolite, biotite, and sillimanite. In the staurolite zone, the occurrence of a wide range of biotite compositions with chlorite, along with other evidence, suggests that chlorite is mainly a retrograde mineral at this grade. A related observation is that the staurolite-chlorite tie line in AFM projection must break early in the staurolite zone; rocks of appropriate composition would form aluminum silicate immediately after staurolite.

4. Staurolite H values are near 3, based on 48 oxygens. Staurolite-garnet and staurolite-biotite K_D plots suggest positive deviation from ideality in Fe-Mg solid solution.

5. Ilmenite is very low in hematite content and coexists with graphite in most pelitic rocks, supporting low f_{O_2} values near QFM.

6. Modified Ganguly-Saxena temperatures indicate that the staurolite-sillimanite rocks in M_3 formed at 581 ± 24 °C and sillimanite–K-feldspar–muscovite rocks in M_5 formed at 659 ± 13 °C.

7. The formation of the first sillimanite from staurolite in M_3, directly above the andalusite field, suggests P = 3.1 ± 0.25 kbar.The muscovite-almandine-biotite-sillimanite (MABS) geobarometer has been calibrated and yields P = 3.8 kbar for M_5.

8. The muscovite breakdown reaction in M_5 is consistent with a T calculated from garnet-biotite, P = 3.8 kbar, and a graphite-present fluid model in which P_{Co_2} is between P_{CH_4} and $10P_{CH_4}$. The staurolite breakdown reaction in M_3 is *not* consistent with garnet-biotite T, but requires a $W_G \approx 15$ kJ per tetrahedral Fe site in order to bring the two sets of data into better agreement. This nonideality suggests a staurolite solvus at about 600 °C.

9. Heat for M_2, M_3, and M_5 came from shallow sill-like batholiths either below or above the present schists. Maximum temperature in M_5 leveled out at about 660 °C (3.8 kbar) due to buffering caused by incipient vapor-absent muscovite melting, ubiquitous local pegmatites and granite, and the Sebago batholith below.

10. Pressure increase from M_2 to M_3 to M_5 (Fig. 8) corresponds to about 5 km over a 75-m.y. period. About half of this is related to a south-southwest movement of the locus of igneous activity and metamorphism and associated P increase with map position. The remainder is a P increase with time that may well be associated with emplacement of shallower intrusive rocks and development of an extensive volcanic highland during the Devonian and Mississippian.

Acknowledgments

We acknowledge with thanks the assistance of Dwight Deuring on the electron microprobe. We thank Jo Ann Weber for writing a computer program to calculate activity coefficients for almandine component. Mary Lee Eggart at LSU drafted the figures. Myrtle Watson is thanked for her expert typing of many drafts of the manuscript. M.J.H. acknowledges the support of the National Science Foundation (grants EAR-8306389 and

EAR-8606489) and B.L.D. the Institute for the Study of Earth and Man at SMU. R.W.H. acknowledges support from NASA (grant NA99-51 to R. N. Clayton). The project has benefited greatly from discussions with C. V. Guidotti and his colleagues at University of Maine and with Darrell Henry at LSU. The manuscript has been reviewed formally by M. P. Dickenson III, Jo Laird, and Eileen McLellan and informally by C. V. Guidotti and Jinny Sisson.

References cited

Albee, A.L., and Ray, L. (1970) Correction factors for electron probe microanalysis of silicates, oxides, carbonates, phosphates, and sulfates. Analytical Chemistry, 42, 1408–1414.

Aleinikoff, J.J., Moench, R.H., and Lyons, J.B. (1985) Carboniferous U-Pb age of the Sebago batholith, southwestern Maine. Geological Society of America Bulletin, 69, 990–996.

Bence, A.E., and Albee, A.L. (1968) Empirical correction factors for electron microanalysis of silicates and oxides. Journal of Geology, 76, 382–403.

Burnham, C.W., Holloway, J.R., and Davis, N.F. (1969) Thermodynamic properties of water to 1,000 °C and 10,000 bars. Geological Society of America Special Paper 132.

Carmichael, D.M. (1978) Metamorphic bathozones and bathograds: A measure of the depth of post-metamorphic uplift and erosion on a regional scale. American Journal of Science, 278, 769–797.

Carnese, M.J. (1983) Gravity studies of intrusive rocks in west-central Maine. M.S. thesis, University of New Hampshire, Durham, New Hampshire.

Chatillon-Colinet, C., Kleppa, O.J., Newton, R.C., and Perkins, D., III. (1983) Enthalpy of formation of $Fe_3Al_2Si_3O_{12}$ (almandine) by high temperature alkali borate solution calorimetry. Geochimica et Cosmochimica Acta, 47, 439–444.

Chatterjee, N.D., and Flux, Susanne. (1986) Thermodynamic mixing properties of muscovite-paragonite crystalline solutions at high temperatures and pressures, and their geological applications. Journal of Petrology, 27, 677–693.

Chatterjee, N.D., and Johannes, Wilhelm. (1974) Thermal stability and standard thermodynamic properties of synthetic $2M_1$-muscovite, $KAl_2[AlSi_3O_{10}(OH)_2]$. Contributions to Mineralogy and Petrology, 48, 89–114.

Cygan, R.T., and Lasaga, A.C. (1982) Crystal growth and the formation of chemical zoning in garnets. Contributions to Mineralogy and Petrology, 79, 187–200.

Dallmeyer, R.D. (1979) Chronology of igneous and metamorphic activity in south-central Maine. In J.W. Skehan and P.H. Osberg, Eds., The Caledonides in the U.S.A., p. 63–71. Weston Observatory, Weston, Massachusetts.

Dallmeyer, R.D., and Vanbreeman, O. (1978) $^{40}Ar/^{39}Ar$ and Rb-Sr ages in west-central Maine; their bearing on the chronology of tectono-thermal events. Geological Society of America Abstracts with Programs, 10, 38.

Dallmeyer, R.D., Vanbreeman, O., and Whitney, J.A. (1982) Rb-Sr whole-rock and $^{40}Ar/^{39}Ar$ mineral ages of the Hartland stock, south-central Maine: A post-Acadian representative of the New Hampshire Plutonic Series. American Journal of Science, 282, 79–93.

DeYoreo, J.J. (1987) The role of crustal anatexis and magma migration in regions of thickened continental crust. Geological Society of America Abstracts with Programs, 19, 10–11.

Dickenson, M.P., and Hewitt, D.A. (1986) A garnet-chlorite geothermometer. Geological Society of America Abstracts with Programs, 18, 584.

Dickerson, R.P. (1984) A study of the polymetamorphism and mineral chemistry of the Little Bigelow Mountain and Bingham quandrangles, Maine. M.S. thesis, Southern Methodist University, Dallas, Texas.

Dutrow, B.L. (1985) A staurolite trilogy: I. Lithium in staurolite and its petrologic significance. II. An experimental determination of the upper stability of staurolite plus quartz. III. Evidence for multiple metamorphic episodes in the Farmington quadrangle, Maine. Ph.D. thesis, Southern Methodist University, Dallas, Texas.

Dutrow, B.L., and Holdaway, M.J. (1983) The upper stability of staurolite + quartz at medium to low pressures. Geological Society of America Abstracts with Programs, 15, 563.

Dutrow, B.L., Holdaway, M.J., and Hinton, R.W. (1986) Lithium in staurolite and its petrologic significance. Contributions to Mineralogy and Petrology, 94, 496–506.

Dymek, R.F. (1983) Titanium, aluminum, and interlayer cation substitutions in biotite from high-grade gneisses, West Greenland. American Mineralogist, 68, 880–899.

Eggleston, R.A., and Bailey, S.W. (1967) Structural aspects of dioctahedral chlorite. American Mineralogist, 52, 673–689.

Evans, B.W. (1969) Chlorine and fluorine in micas of pelitic schists from the sillimanite-orthoclase isograd, Maine. American Mineralogist, 54, 1209–1211.

Evans, B.W., and Guidotti, C.V. (1966) The sillimanite–potash feldspar isograd in western Maine, U.S.A. Contributions to Mineralogy and Petrology, 12, 25–62.

Ferry, J.M. (1976) P, T, f_{CO_2}, and f_{H_2O} during metamorphism of calcareous sediments in the Waterville-Vassalboro area, south-central Maine. Contributions to Mineralogy and Petrology, 57, 119–143.

——— (1980) A case study of the amount and distribution of heat and fluid during metamorphism. Contributions to Mineralogy and Petrology, 71, 373–385.

Ferry, J.M., and Spear, F.S. (1978) Experimental calibration of partitioning of Fe and Mg between biotite and garnet. Contributions to Mineralogy and Petrology, 66, 113–117.

Fyfe, W.S., Turner, F.J., and Verboogen, J. (1958) Metamorphic reactions and metamorphic facies. Geological Society of America Memoir 73.

Ganguly, Jibamitra. (1969) Chloritoid stability and related parageneses: Theory, experiments, and applications. American Journal of Science, 267, 910–944.

Ganguly, Jibamitra, and Saxena, S.K. (1984) Mixing properties of aluminosilicate garnets: Constraints from natural and experimental data, and applications to geothermobarometry. American Mineralogist, 69, 88–97.

——— (1985) Mixing properties of aluminosilicate garnets: Constraints from natural and experimental data, and applications to geothermobarometry: Clarifications. American Mineralogist, 70, 1320.

Gaudette, H.E., and Boone, G.M. (1985) Isotopic age of the Lexington batholith: Constraints on timing of Acadian metamorphism in western Maine. Geological Society of America Abstracts with Programs, 17, 19–20.

Geving, R.L. (1987) A study of the metamorphic petrology of the northern Snake Range, east-central Nevada. M.S. thesis, Southern Methodist University, Dallas, Texas.

Grambling, J.A. (1983) Reversals in Fe-Mg partitioning between chloritoid and staurolite. American Mineralogist 68, 373–388.

Guidotti, C.V. (1968) Prograde muscovite pseudomorphs after staurolite in the Rangeley-Oquossoc area, Maine. American Mineralogist, 53, 1368–1376.

——— (1970) Metamorphic petrology, mineralogy, and polymetamorphism in a portion of northwest Maine. New England Intercollegiate Geological Conference, 62nd Annual Meeting, B-2, 1–23.

——— (1974) Transition from staurolite to sillimanite zone, Rangeley quadrangle, Maine. Geological Society of America Bulletin, 85, 475–490.

——— (1978) Compositional variation of muscovite in medium- to high-grade metapelites of northwestern Maine. American Mineralogist, 63, 878–884.

——— (1984) Micas in metamorphic rocks. Mineralogical Society of America Reviews in Mineralogy, 13, 357–467.

Guidotti, C.V., Herd, H.H., and Tuttle, C.L. (1973) Composition and structural state of K-feldspar from K-feldspar + sillimanite grade rocks in northwestern Maine. American Mineralogist, 58, 705–716.

Guidotti, C.V., Trzcienski, W.E., and Holdaway, M.J. (1983) A northern Appalachian metamorphic transect—Eastern townships, Quebec-Maine coast to the central Maine coast. In P.E. Schenk, Ed., Regional trends in the geology of the Appalachian-Caledonian-Mauritanide orogen, p. 235–247. Reidel, Boston, Massachusetts.

Guidotti, C.V., Gibson, D., Lux, D.R., DeYoreo, J.J., and Cheney, J.T. (1986) Carboniferous metamorphism on the north (upper) side of the

Sebago batholith. New England Intercollegiate Conference, 78th Annual Meeting, 306–341.

Hayward, J.A., and Gaudette, H.E. (1984) Carboniferous age of the Sebago and Effingham plutons, Maine and New Hampshire, Geological Society of America Abstracts with Programs, 16, 22.

Helgeson, H.C., Delany, J.M., Nesbitt, H.W., and Bird, D.K. (1978) Summary and critique of the thermodynamic properties of rock-forming minerals. American Journal of Science, 278-A.

Hemingway, B.S., and Robie, R.A. (1984) Heat capacity and thermodynamic functions for gehlenite and staurolite: With comments on the Schottky anomaly in the heat capacity of staurolite. American Mineralogist, 69, 307–318.

Henry, W.E. (1974) Metamorphism of the pelitic schists in the Dixfield quadrangle, NW Maine. Ph.D. thesis, University of Wisconsin, Madison, Wisconsin.

Hodge, D.S., Abbey, D.A., Hasbin, M.A., Patterson, J.L., Ring, M.J., and Sweeney, J.F. (1982) Gravity studies of subsurface mass distributions of granitic rocks in Maine and New Hampshire. American Journal of Science, 282, 1289–1324.

Hodges, K.V., and Spear, F.S. (1982) Geothermometry, geobarometry and the Al_2SiO_5 triple point at Mt. Moosilauke, New Hampshire. American Mineralogist, 67, 1118–1134.

Holdaway, M.J. (1971) Stability of andalusite and the aluminum silicate phase diagram. American Journal of Science, 271, 97–131.

——— (1978) Significance of chloritoid-bearing and staurolite-bearing rocks in the Picuris Range, New Mexico. Geological Society of America Bulletin, 89, 1404–1414.

——— (1980) Chemical formulae and activity models for biotite, muscovite, and chlorite applicable to pelitic metamorphic rocks. American Mineralogist, 65, 711–719.

Holdaway, M.J., Guidotti, C.V., Novak, J.M., and Henry, W.E. (1982) Polymetamorphism in medium- to high-grade pelitic metamorphic rocks, west-central Maine. Geological Society of America Bulletin, 93, 572–584.

Holdaway, M.J., Dickerson, R.P., and Dutrow, B.L. (1986a) Petrology and field relations of M2 metamorphism in west-central Maine. New England Intercollegiate Geological Conference, 78th Annual Meeting, 240–253.

Holdaway, M.J., Dutrow, B.L., and Shore, Patrick. (1986b) A model of the crystal chemistry of staurolite. American Mineralogist, 71, 1142–1159.

Holdaway, M.J., Dutrow, B.L., Borthwick, James, Shore, Patrick, Harmon, R.S., and Hinton, R.W. (1986c) H content of staurolite as determined by H extraction line and ion microprobe. American Mineralogist, 71, 1135–1141.

Hussey, A.M., Bothner, W.A., and Thomson, J.A. (1986) Geological comparisons across the Norumbega fault zone, southwestern Maine. New England Intercollegiate Geological Conference, 78th Annual Meeting, 53–78.

Jones, A.P., and Smith, J.V. (1984) Ion probe analysis of H, Li, B, F, and Ba in micas, with additional data for metamorphic amphibole, scapolite, and pyroxene. Neues Jahrbuch für Mineralogie Monatshefte, 228–240.

Juurinen, Aarno. (1956) Composition and properties of staurolite. Annales Academiae Scientiarum Fennicae, Series A, III Geology, 47, 1–53.

Kerrick, D.M. (1972) Experimental determination of muscovite + quartz stability with $P_{H_2O} < P_{total}$. American Journal of Science, 272, 946–958.

——— (1974) Review of mixed-volatile (H_2O-CO_2) equilibria. American Mineralogist, 59, 729–762.

Kerrick, D.M., and Jacobs, G.K. (1981) A modified Redlich-Kwong equation for H_2O, CO_2, and H_2O-CO_2 mixtures at elevated pressures and temperatures. American Journal of Science, 281, 735–767.

Kretz, Ralph. (1983) Symbols for rock-forming minerals. American Mineralogist, 68, 277–279.

Lux, D.R., and Guidotti, C.V. (1985) Evidence for extensive Hercynian metamorphism in western Maine. Geology, 13, 695–700.

Lux, D.R., DeYoreo, J.J., Guidotti, C.V., and Decker, E.R. (1986) Role of plutonism in low-pressure metamorphic belt formation. Nature, 323, 794–797.

McLellan, Eileen. (1985) Metamorphic reactions in the kyanite and sillimanite zones of the Barrovian type area. Journal of Petrology, 26, 789–818.

Metz, G.W., Anovitz, L.M., Essene, E.J., Bohlen, S.R., Westrum, E.F., and Wall, V.J. (1983) The heat capacity and phase equilibria of almandine (abs.). EOS, 64, 346–347.

Moench, R.H., and Zartman, R.E. (1976) Chronology and styles of multiple deformation, plutonism, and polymetamorphism in the Merrimack synclinorium of western Maine. In P.C. Lyons and A.H. Brownlow, Eds., Studies in New England geology. Geological Society of America Memoir 146, 203–238.

Munoz, J.L., and Ludington, S.D. (1974) Fluorine-hydroxyl exchange in biotite. American Journal of Science, 274, 396–413.

——— (1977) Fluorine-hydroxyl exchange in synthetic muscovite and its application to muscovite-biotite assemblages. American Mineralogist, 62, 304–308.

Newton, R.C., and Haselton, H.T. (1981) Thermodynamics of the garnet-plagioclase-Al_2SiO_5-quartz geobarometer. In R.C. Newton et al., Eds., Advances in physical geochemistry, vol. 1, p. 111–147. Springer-Verlag, New York.

Novak, J.M., and Holdaway, M.J. (1981) Metamorphic petrology, mineral equilibria, and polymetamorphism in the Augusta quadrangle, south-central Maine. American Mineralogist, 66, 51–69.

Ohmoto, Hiroshi, and Kerrick, D.M. (1977) Devolatilization equilibria in graphitic systems. American Journal of Science, 277, 1013–1044.

Osberg, P.H., Hussey, A.M., and Boone, G.M. (1985) Bedrock geologic map of Maine. Maine Geological Survey, Augusta, Maine.

Pigage, L.C., and Greenwood, H.J. (1982) Internally consistent estimates of pressure and temperature: The staurolite problem. American Journal of Science, 282, 943–969.

Powell, Roger, and Evans, J.A. (1983) A new geobarometer for the assemblage biotite-muscovite-chlorite-quartz. Journal of Metamorphic Geology, 1, 331–336.

Rankin, D.W. (1968) Volcanism related to tectonism in the Piscataquis volcanic belt, an island arc of Early Devonian age in north-central Maine. In E-an Zen et al., Eds., Studies of Appalachian geology: Northern and maritime, p. 355–369. Interscience, New York.

Rice, J.M. (1985) Experimental partitioning of Fe and Mg between coexisting staurolite and garnet (abs.). EOS, 66, 1127.

Richardson, S.W. (1966) Staurolite. Carnegie Institution of Washington Yearbook, 65, 248–252.

——— (1968) Staurolite stability in a part of the system Fe-Al-Si-O-H. Journal of Petrology, 9, 467–488.

Robie, R.A., and Hemingway, B.S. (1984) Entropies of kyanite, andalusite, and sillimanite: Additional constraints on the pressure and temperature of the Al_2SiO_5 triple point. American Mineralogist, 69, 298–306.

Robinson, G.R., Jr. (1983) Calibration of the muscovite-biotite-quartz-garnet-aluminosilicate geothermobarometer (abs.). EOS, 64, 351.

Ryzhenko, B.N., and Volkov, V.P. (1971) Fugacity coefficients of some gases in a broad range of temperatures and pressures. Geochemistry International, 8, 468–481.

Schreyer, Werner, and Seifert, F. (1969) Compatibility relations of the aluminum silicates in the systems MgO-Al_2O_3-SiO_2-H_2O and K_2O-MgO-Al_2O_3-SiO_2-H_2O at high pressures. American Journal of Science, 267, 407–443.

Schreyer, Werner, Horrocks, P.C., and Abraham, K. (1984) High-magnesium staurolite in a sapphirine-garnet rock from the Limpopo belt, southern Africa. Contributions to Mineralogy and Petrology, 86, 200–207.

Smith, J.V. (1968) The crystal structure of staurolite. American Mineralogist, 53, 1139–1155.

Spear, F.S., and Selverstone, Jane. (1983) Quantitative P-T paths from zoned minerals: Theory and tectonic applications. Contributions to Mineralogy and Petrology, 83, 348–357.

Speer, J.A. (1984) Micas in igneous rocks. Mineralogical Society of America Reviews in Mineralogy, 13, 299–356.

Steele, J.M., Hervig, R.L., Hutcheon, I.D., and Smith, J.V. (1981) Ion microprobe techniques and analysis of olivines and low-calcium pyroxenes. American Mineralogist, 66, 526–546.

Thompson, A.B. (1976) Mineral reactions in pelitic rocks: I. Prediction of *P-T-X*(Fe-Mg) phase relations. American Journal of Science, 276, 401–424.

Thompson, J.B. (1982) Composition space: An algebraic and geometric approach. Mineralogical Society of America Reviews in Mineralogy, 10, 1–31.

Thomson, J.A., and Guidotti, C.V. (1986) The occurrence of kyanite in southern Maine and its metamorphic implications. Geological Society of America Abstracts with Programs, 17, 59.

Tompkins, L.A., Bailey, S.W., and Haggerty, S.E. (1984) Kimberlitic chlorites from Sierra Leone, West Africa: Unusual chemistries and structural polytypes. American Mineralogist, 69, 237–249.

Tracy, R.J. (1978) High grade metamorphic reactions and partial melting in pelitic schists, west-central Massachusetts. American Journal of Science, 278, 150–178.

——— (1982) Compositional zoning and inclusions in metamorphic minerals. Mineralogical Society of America Reviews in Mineralogy, 10, 355–397.

Veblen, D.R. (1983) Microstructures and mixed layering in intergrown wonesite, chlorite, talc, biotite, and kaolinite. American Mineralogist, 68, 566–580.

Velde, B. (1965) Phengite micas: Synthesis, stability and natural occurrence. American Journal of Science, 263, 886–913.

Waldbaum, D.R., and Thompson, J.B., Jr. (1969) Mixing properties of sanidine crystalline solutions: IV. Phase diagrams from equations of state. American Mineralogist, 54, 1274–1298.

Zen, E-an. (1981) Metamorphic mineral assemblages of slightly calcic pelitic rocks in and around the Taconic allochthon, southwestern Massachusetts and adjacent Connecticut and New York. U.S. Geological Survey Professional Paper 1113.

Manuscript received March 20, 1987
Manuscript accepted September 14, 1987

Appendix 1. Staurolite data

Entropy

Hemingway and Robie (1984) have provided entropy data for staurolite 355-1, originally studied by Zen (1981).

Chemical correction. Holdaway et al. (1986b) have shown that this staurolite has the formula $H_{3.32}(Fe_{3.36}Mg_{0.458}Mn_{0.028}Zn_{0.052}Li_{0.326}Cr_{0.013}Co_{0.02}Ti_{0.084})Al_{17.757}Si_{7.713}O_{48}$.[6] In order to correct for the chemical differences between this staurolite and pure Fe "end-member" staurolite ($H_3Fe_{4.3}Al_{17.92}Si_{7.66}O_{48}$) as used in Reaction 8, appropriate amounts of entropy of the following compounds were added or subtracted from the raw data of Hemingway and Robie (1984): MgO, Li_2O, pyrophyllite, Cr_2O_3, ZnO, TiO_2, MnO, CoO, SiO_2, Al_2O_3, and fayalite. The molar volumes of the subtracted components summed to 3.114 J/bar, and the sum for the added components was 3.055 J/bar. This slight compression was corrected for by subtracting 1.48 J/K from the entropy (25.1 J/K for each J/bar; Fyfe et al., 1958). The total chemical correction was +23.47 − 1.48 = +21.99 J/K.

[6] Co is given as 0.02 to account for small amounts of Co, V, and Zr.

Disorder correction. In order to make the disorder correction, two assumptions were made: (1) The staurolite is as ordered as possible, i.e., minimum corrections were made; (2) the corrections that were made are corrections that can be reasonably assumed to be constant for Fe "end-member" staurolite *and* for the natural staurolites from west-central Maine. The "end-member" staurolite formula may be rewritten as $(H_3\square_1)_4(Fe_{3.9}\square_{0.1})_4(Al_{1.58}Fe_{0.15}\square_{0.27})_2(Fe_{0.25}\square_{1.75})_2Al_{16}(Si_{7.66}Al_{0.34})_8O_{48}$. Following the maximum-order structure model of Holdaway et al. (1986b) with P(1B), Al(3A), U(1) sites partially filled and P(1A), Al(3B), and U(2) sites empty, we have the following disorder terms with $\Delta S_{mix} = -R[(X \ln X) + ((1 - X)\ln(1 - X))]$ per site: (1) ^{iv}Fe site disorder is $-4R[0.025 \ln 0.025 + 0.975 \ln 0.975] = 0.4676R$. (2) P(1B) site disorder involves only 3.95 sites and 2.9 ions because 0.05 H each on P(1A) and P(1B) is coupled to the 0.1 vacancy in ^{iv}Fe. Disorder is $-3.95R[0.734 \ln 0.734 + 0.266 \ln 0.266] = 2.2880R$. (3) Al(3A) site disorder includes U(1) disorder to which it is coupled. Disorder is $-2R[0.790 \ln 0.790 + 0.075 \ln 0.075 + 0.135 \ln 0.135] = 1.3017R$. (4) Si site disorder is $-8R[0.958 \ln 0.958 + 0.042 \ln 0.042] = 1.4065R$. Total disorder entropy is $5.4638R = 45.42$ J/K.

Hemingway and Robie's (1984) Table 6, which already has a +121.0-J/K chemical and disorder correction, may be adapted to the present Fe "end-member" staurolite by subtracting 53.59 J/K (−121.0 + 21.99 + 45.42).

Activity model

Because the above disorder corrections apply to the Fe "end-member" staurolite in hydrothermal experiments and in nature, none of them should be taken into account in the activity model. In determining the model and calculating staurolite activities, the following reasonable assumptions were made (Juurinen, 1956; Holdaway et al., 1986b). (1) Assume that the H content of the staurolites is 3 and fix the ^{iv}Fe site vacancy at 0.1 ions pfu. Thus ^{iv}Fe occupancy totals 3.9 (to allow this quantity to vary in these specimens would produce variations resulting largely from analytical error). (2) 0.25 (Mn + Fe) pfu is assigned to U(1) and 0.15 Fe pfu is assigned to Al(3A). Where Li is not known, an average value of 0.3 pfu is assumed. Remaining Fe, Mg, Zn, and Li are assigned to ^{iv}Fe sites.

The activity model below restricts additional solid solution to the ^{iv}Fe and U(1) sites (i = end-member values):

$$\frac{{}^{iv}X_{Fe}^{3.9} \times {}^{iv}X_{\square,i}^{0.1} \times {}^{U}X_{Fe}^{0.25} \times {}^{U}X_{\square,i}^{1.75}}{{}^{iv}X_{Fe,i}^{3.9} \times {}^{iv}X_{\square,i}^{0.1} \times {}^{U}X_{Fe,i}^{0.25} \times {}^{U}X_{\square,i}^{1.75}} = {}^{iv}X_{Fe}^{3.9} \times {}^{U}X_{Fe}^{0.25}.$$

The mole fractions are based on the analytical quantities, per 48 oxygens:

$${}^{iv}X_{Fe} = \frac{Fe + Mn - 0.4}{R^{2+} + Li - 0.4}; \quad {}^{U}X_{Fe} = \frac{0.25 - Mn}{0.25}.$$

The value 0.4 corrects for Mn and Fe in the U(1) and Al(3A) sites (0.25 and 0.15, respectively).

APPENDIX TABLE 1. Stoichiometric compositions of minerals[a]

	Grade	3		*				4						*			5			*	6	
	Specimen	2	96	1A	52	3A	61A	84	129	114	5A	65	94	27	137	53	14A	6	23	79	4A	
Muscovite	Si	6.090	6.045	6.059	6.002	6.018	6.049	6.112	6.063	6.050	6.045	6.080	6.055	6.036	6.083	6.051	6.014	6.015	6.013	6.017	6.034	
	Al	5.636	5.792	5.706	5.874	5.826	5.768	5.675	5.777	5.812	5.734	5.704	5.762	5.815	5.701	5.737	5.800	5.776	5.785	5.786	5.727	
	Ti	0.031	0.023	0.043	0.023	0.031	0.027	0.027	0.023	0.027	0.043	0.043	0.035	0.020	0.047	0.047	0.040	0.043	0.059	0.062	0.047	
	Fe	0.154	0.103	0.114	0.078	0.089	0.091	0.122	0.082	0.078	0.106	0.102	0.101	0.110	0.110	0.098	0.106	0.105	0.094	0.102	0.114	
	Mg	0.186	0.079	0.122	0.074	0.085	0.095	0.110	0.090	0.070	0.118	0.105	0.093	0.059	0.098	0.098	0.083	0.117	0.090	0.078	0.134	
	K	1.627	1.599	1.679	1.444	1.490	1.625	1.625	1.533	1.418	1.670	1.662	1.542	1.524	1.559	1.546	1.594	1.669	1.590	1.540	1.727	
	Na	0.252	0.336	0.255	0.488	0.409	0.328	0.264	0.388	0.490	0.248	0.235	0.367	0.406	0.362	0.404	0.356	0.247	0.334	0.387	0.225	
	Ba	0.008	0.004	0.012	0.007	0.019	0.004	0.008	0.008	0.027	0.016	0.012	0.007	0.012	0.008	0.012	0.016	0.016	0.012	0.008	0.016	
	Σ(Ox)	94.14	93.54	94.71	94.54	94.89	93.60	94.12	94.24	94.03	94.56	94.59	94.75	93.97	94.09	94.43	93.88	94.88	94.23	94.74	94.56	
Biotite	Si	5.420	5.421	5.386	5.405	5.411	5.404	5.400	5.362	5.415	5.375	5.279	5.425	5.337	5.384	5.394	5.373	5.406	5.353	5.348	5.375	
	Al	3.394	3.452	3.514	3.505	3.530	3.490	3.530	3.548	3.544	3.541	3.569	3.523	3.625	3.507	3.514	3.516	3.517	3.531	3.591	3.534	
	Ti	0.186	0.179	0.166	0.174	0.159	0.144	0.164	0.167	0.161	0.183	0.182	0.163	0.203	0.203	0.193	0.209	0.278	0.245	0.158	0.264	
	Fe	2.236	2.789	2.195	2.439	2.209	2.257	2.691	2.636	2.611	2.261	2.783	2.507	3.174	2.490	2.522	2.684	2.310	2.654	2.848	2.199	
	Mg	2.527	1.938	2.495	2.252	2.473	2.497	1.979	2.101	2.067	2.370	2.101	2.109	1.416	2.140	2.127	1.947	2.157	1.958	1.811	2.318	
	Mn	0.027	0.009	0.013	0.009	0.013	0.018	0.022	0.004	0.004	0.011	0.005	0.009	0.004	0.009	0.009	0.018	0.013	0.009	0.009	0.013	
	K	1.762	1.712	1.783	1.650	1.637	1.758	1.697	1.628	1.616	1.774	1.560	1.694	1.694	1.721	1.669	1.706	1.724	1.713	1.698	1.723	
	Na	0.050	0.027	0.058	0.080	0.101	0.041	0.055	0.054	0.085	0.057	0.059	0.085	0.087	0.088	0.085	0.082	0.031	0.059	0.095	0.057	
	Σ(Ox)	94.23	93.16	94.12	94.76	95.27	93.11	93.70	93.72	93.88	94.45	93.98	93.86	94.26	93.87	94.49	93.95	93.68	94.30	94.84	95.44	
Garnet Cores	alm	0.554	0.654	0.556	0.698	0.687	0.654	0.683	0.735	0.810	0.658	0.731	0.732	0.841	0.781	0.764	0.731	0.673	0.748	0.763	0.604	
	prp	0.078	0.051	0.068	0.081	0.107	0.101	0.066	0.081	0.094	0.106	0.078	0.100	0.059	0.109	0.109	0.084	0.113	0.105	0.065	0.103	
	sps	0.333	0.247	0.286	0.174	0.167	0.204	0.218	0.128	0.035	0.168	0.124	0.116	0.074	0.076	0.094	0.169	0.144	0.106	0.123	0.211	
	grs	0.035	0.048	0.090	0.048	0.038	0.041	0.033	0.055	0.060	0.069	0.067	0.052	0.026	0.034	0.034	0.016	0.070	0.041	0.049	0.083	
	Σ(Ox)	99.78	98.49	99.92	100.46	100.42	99.40	98.95	100.73	99.40	100.39	99.69	99.80	100.46	99.73	100.74	100.15	99.80	100.37	100.18	100.86	
Garnet Intermed.	alm	0.600	0.683	0.671	0.750	0.687	0.665	0.683	0.790	0.817	0.666	0.748	0.732	0.862	0.788	0.769	0.733	0.676	0.760	0.769	0.632	
	prp	0.087	0.057	0.104	0.095	0.107	0.101	0.066	0.084	0.091	0.109	0.084	0.100	0.063	0.100	0.104	0.077	0.166	0.099	0.067	0.112	
	sps	0.279	0.210	0.150	0.117	0.167	0.190	0.218	0.067	0.032	0.161	0.098	0.116	0.053	0.080	0.092	0.169	0.139	0.110	0.113	0.184	
	grs	0.034	0.050	0.075	0.038	0.038	0.044	0.033	0.059	0.060	0.065	0.069	0.052	0.022	0.032	0.035	0.021	0.069	0.031	0.051	0.072	
	Σ(Ox)	99.83	99.21	100.41	100.71	100.42	99.36	98.95	99.94	99.52	100.45	100.52	99.80	100.32	100.26	100.65	100.19	100.79	100.49	100.48	100.91	
Staurolite	Si			7.621	7.632	7.638	7.578	7.699	7.592	7.621	7.734	7.660	7.581	7.506	7.703	7.506	7.617	7.823	7.595			
	Al			17.909	17.898	17.911	17.952	17.831	17.938	17.891	17.796	17.870	17.949	18.024	17.827	18.006	17.913	17.898	17.935			
	Ti			0.110	0.090	0.114	0.103	0.080	0.097	0.093	0.114	0.086	0.104	0.080	0.106	0.105	0.119	0.083	0.115			
	Fe			3.036	3.408	3.300	3.126	3.121	3.374	3.383	3.201	3.418	3.422	3.662	3.283	3.441	3.008	2.509	3.249			
	Mg			0.610	0.661	0.790	0.623	0.465	0.577	0.561	0.683	0.567	0.590	0.443	0.586	0.609	0.519	0.374	0.560			
	Mn			0.082	0.038	0.114	0.101	0.121	0.029	0.017	0.076	0.045	0.040	0.017	0.045	0.054	0.079	0.101	0.054			
	Zn			0.069	0.060	0.037	0.039	0.270	0.064	0.060	0.230	0.037	0.062	0.062	0.083	0.050	0.407	0.202	0.173			
	Li			n.d.	n.d.	n.d.	n.d.	n.d.	n.d.	0.418	n.d.	n.d.	n.d.	n.d.	n.d.	0.259	n.d.	0.993[c]	n.d.			
	H			3.755[b]	3.084	2.677	3.642	3.437	3.342	2.903	2.840	3.272	3.185	3.216	3.289	2.969	3.291	3.312	3.283			
	Σ(Ox)			100.31	100.61	100.10	99.79	99.63	99.75	99.84	99.99	100.09	99.85	100.54	99.46	100.51	99.21	99.87	100.60			
Chlorite	Si	5.225	5.157		5.131	5.131	5.172	5.156	5.143	5.123			5.105	5.142								
	Al	5.649	5.808		5.801	5.793	5.714	5.770	5.771	5.856			5.814	5.828								
	Ti	0.012	0.013		0.012	0.012	0.012	0.025	0.012	0.006			0.012	0.013								
	Fe	3.887	5.029		4.282	3.838	3.995	4.871	4.710	4.731			4.516	5.847								
	Mg	5.065	3.887		4.697	5.107	5.010	4.030	4.296	4.193			4.484	3.065								
	Mn	0.061	0.019		0.012	0.042	0.037	0.057	0.012	0.006			0.019	0.006								
	Ca	0.006	0.000		0.006	0.000	0.000	0.000	0.000	0.000			0.000	0.000								
	Σ(Ox)	86.89	86.28		87.04	86.86	85.91	86.72	87.04	86.29			86.55	86.98								
Ilmenite	ilm	0.906	0.973	0.955	0.974	0.948	0.929	P	0.977	0.982	0.963	0.970	0.961	0.994	0.972	0.977	0.941	0.939	0.971	0.976	0.928	
	pyr	0.094	0.027	0.045	0.019	0.052	0.050		0.013	0.005	0.030	0.022	0.018	0.006	0.018	0.022	0.059	0.060	0.027	0.024	0.060	
	gei	0.000	0.000	0.000	0.000	0.000	0.001		0.000	0.003	0.000	0.000	0.006	0.000	0.000	0.001	0.000	0.001	0.001	0.000	0.005	
	hem	0.000	0.000	0.000	0.007	0.000	0.020		0.010	0.010	0.007	0.008	0.015	0.000	0.010	0.000	0.000	0.000	0.001	0.000	0.007	
	Σ(Ox)	98.44	98.98	98.66	99.62	98.15	98.68		98.80	99.24	99.64	98.89	99.41	98.92	99.92	98.61	97.92	97.36	98.49	98.54	98.99	
Plag.	an	P										P						0.388	P	P	0.340	
	ab																	0.611			0.658	
	or																	0.001			0.002	
	Σ(Ox)																	100.58			100.48	

APPENDIX TABLE 1—*Continued*

	Grade	6								*			6.5			*		7			*	8
	Specimen	47	19	112	50	63	30	8	140	77-3	77-2	90	76	56	91	73	87	143	145	86	11
Muscovite	Si	6.060	6.016	6.014	6.027	6.053	6.051	6.063	6.037	6.053	6.026	6.037	6.071	6.063	6.036	6.055	6.073	6.072	6.055	6.072	6.038
	Al	5.704	5.743	5.778	5.770	5.700	5.697	5.603	5.716	5.666	5.716	5.706	5.679	5.705	5.680	5.630	5.632	5.652	5.631	5.666	5.653
	Ti	0.048	0.063	0.063	0.048	0.065	0.055	0.075	0.067	0.081	0.081	0.083	0.072	0.064	0.091	0.103	0.074	0.071	0.108	0.060	0.111
	Fe	0.110	0.115	0.090	0.106	0.115	0.110	0.154	0.115	0.115	0.110	0.114	0.117	0.110	0.134	0.125	0.131	0.117	0.126	0.134	0.118
	Mg	0.126	0.103	0.098	0.099	0.107	0.118	0.150	0.107	0.119	0.114	0.122	0.125	0.098	0.103	0.125	0.130	0.108	0.110	0.118	0.125
	K	1.668	1.646	1.585	1.585	1.717	1.748	1.782	1.717	1.702	1.666	1.674	1.749	1.698	1.792	1.816	1.875	1.840	1.816	1.811	1.853
	Na	0.265	0.301	0.326	0.328	0.206	0.205	0.163	0.206	0.258	0.251	0.236	0.137	0.236	0.150	0.137	0.083	0.126	0.130	0.114	0.090
	Ba	0.008	0.016	0.008	0.008	0.012	0.016	0.020	0.012	0.016	0.020	0.008	0.004	0.000	0.008	0.008	0.004	0.004	0.012	0.008	0.008
	Σ(Ox)	93.96	94.07	94.18	93.71	93.81	94.68	94.32	93.81	93.95	94.79	94.36	94.93	94.27	94.42	95.04	94.56	94.46	94.38	94.75	95.26
Biotite	Si	5.372	5.361	5.397	5.369	5.365	5.361	5.376	5.374	5.366	5.354	5.354	5.343	5.353	5.325	5.351	5.344	5.331	5.349	5.312	5.359
	Al	3.527	3.465	3.727	3.489	3.467	3.526	3.396	3.397	3.473	3.445	3.409	3.412	3.386	3.435	3.413	3.456	3.446	3.485	3.457	3.505
	Ti	0.168	0.243	0.217	0.298	0.265	0.257	0.326	0.271	0.292	0.281	0.337	0.360	0.335	0.399	0.419	0.356	0.346	0.407	0.364	0.331
	Fe	2.343	2.633	2.402	2.693	2.725	2.425	2.298	2.579	2.463	2.529	2.531	2.543	2.605	2.658	2.443	2.511	2.549	2.584	2.579	2.328
	Mg	2.357	2.054	1.855	1.830	1.875	2.064	2.244	2.090	2.050	2.087	1.986	1.967	1.959	1.749	1.878	1.897	1.898	1.679	1.899	2.050
	Mn	0.009	0.013	0.023	0.004	0.013	0.027	0.013	0.013	0.013	0.013	0.022	0.018	0.020	0.022	0.022	0.009	0.018	0.013	0.009	0.013
	K	1.711	1.709	1.698	1.712	1.796	1.812	1.843	1.746	1.772	1.738	1.779	1.805	1.834	1.872	1.872	1.911	1.939	1.896	1.891	1.862
	Na	0.071	0.072	0.073	0.072	0.054	0.062	0.049	0.086	0.067	0.071	0.067	0.045	0.052	0.036	0.044	0.027	0.036	0.036	0.027	0.031
	Σ(Ox)	94.84	94.79	93.93	94.69	94.50	95.49	94.96	94.35	94.65	95.22	94.69	94.86	94.73	94.59	95.45	94.61	94.19	94.70	95.25	94.65
Garnet Cores	alm	0.663	0.709	0.691	0.764	0.711	0.629	0.641	0.673	0.710	0.704	0.681	0.685	0.704	0.696	0.675	0.731	0.751	0.766	0.778	0.702
	prp	0.119	0.099	0.096	0.099	0.091	0.101	0.131	0.112	0.121	0.123	0.112	0.112	0.112	0.102	0.108	0.126	0.130	0.114	0.145	0.180
	sps	0.166	0.168	0.181	0.115	0.150	0.219	0.172	0.185	0.143	0.147	0.187	0.177	0.146	0.177	0.184	0.082	0.091	0.099	0.062	0.055
	grs	0.052	0.024	0.032	0.022	0.048	0.051	0.056	0.029	0.025	0.025	0.020	0.026	0.038	0.024	0.033	0.061	0.028	0.021	0.015	0.063
	Σ(Ox)	100.89	100.04	100.54	100.06	100.05	101.73	100.94	99.99	101.00	101.02	99.91	100.15	100.37	99.51	100.32	100.10	99.48	100.04	100.34	100.85
Garnet Intermed.	alm	0.674	0.739	0.695	0.785	0.719	0.642	0.662	0.701	0.725	0.719	0.698	0.706	0.719	0.713	0.681	0.734	0.750	0.766	0.783	0.717
	prp	0.112	0.096	0.084	0.096	0.084	0.093	0.128	0.106	0.115	0.116	0.112	0.107	0.102	0.097	0.101	0.115	0.114	0.114	0.128	0.161
	sps	0.165	0.139	0.201	0.099	0.148	0.218	0.151	0.165	0.133	0.138	0.170	0.162	0.141	0.167	0.187	0.089	0.107	0.099	0.073	0.062
	grs	0.050	0.026	0.020	0.020	0.049	0.047	0.059	0.029	0.027	0.027	0.020	0.025	0.038	0.023	0.032	0.062	0.029	0.021	0.015	0.060
	Σ(Ox)	101.06	100.52	100.25	100.45	100.30	101.49	100.68	100.28	100.80	100.92	99.48	100.54	100.38	100.05	100.63	100.32	99.43	100.04	100.57	101.21
Orthoclase	or															0.840	0.899	0.862	0.835	0.883	0.888
	ab															0.152	0.093	0.129	0.146	0.101	0.101
	an															0.000	0.000	0.000	0.000	0.000	0.000
	cs															0.008	0.008	0.009	0.018	0.016	0.011
	(Ox)															100.39	99.94	99.58	99.30	99.76	99.77
Ilmenite	ilm	0.957	0.969	0.909	0.978	0.896	0.887	0.891	0.968	0.961	0.952		0.933	0.954			P	P		P	
	pyr	0.041	0.028	0.068	0.017	0.067	0.111	0.086	0.032	0.026	0.027		0.066	0.044							
	gei	0.000	0.003	0.001	0.000	0.000	0.000	0.001	0.000	0.003	0.003		0.000	0.000							
	hem	0.002	0.000	0.022	0.005	0.037	0.002	0.022	0.000	0.010	0.018		0.001	0.002							
	Σ(Ox)	99.49	99.55	99.92	99.59	100.97	99.15	100.29	99.45	99.85	100.70		99.25	98.99							
Plag.	an	0.293	0.166	P		0.297	0.314	0.389	0.181	0.179	0.180	P	0.195	0.265	0.157	0.230	0.529	P	P	0.115	0.479
	ab	0.705	0.832			0.701	0.683	0.608	0.817	0.817	0.817		0.798	0.732	0.836	0.761	0.463			0.879	0.515
	or	0.002	0.002			0.002	0.003	0.003	0.002	0.004	0.003		0.007	0.003	0.007	0.009	0.008			0.006	0.006
	Σ(Ox)	100.88	100.39			100.65	100.78	101.09	99.73	99.92	100.47		100.49	100.35	100.53	100.25	100.41			100.10	100.94

[a] Stoichiometry is based on 22 oxygens for micas, endmember proportions for garnets, feldspars, and ilmenite, 28 oxygens for chlorite, and 25.53 (Si+Al) for staurolite. P indicates mineral present but not abundant enough for analysis. A after number indicates specimen contains M_2 andalusite.
[b] Values underlined are approximate calculated values for (H+Li) and Σ(Ox). If Li is assumed to be 0.3 pfu, the remainder is an approximate indication of H.
[c] Li content of this staurolite is about 1.39 pfu and variable. The number used here is from a more accurate AA analysis from an otherwise identical staurolite from the same outcrop (Dutrow et al., 1986).

Note added in proof. We have recently observed that the four andalusite-bearing rocks of grade 4 (App. Table 1, Fig. 1) from the Augusta quadrangle are compositionally distinct from all other rocks in grade 4. These andalusite-bearing rocks contain higher Mg/Fe in staurolite, biotite, and garnet and higher spessartine + grossular in garnet, indicating that they represent the compositional limit of staurolite stability. Because these specimens are compositionally unique, the andalusite need not have an M_2 origin. Other evidence (e.g., local cordierite) suggests increasing *P* during metamorphism. Novak and Holdaway (1981) suggested that M_2 and M_3 tend to merge in time and metamorphic conditions in this area. The probability that andalusite formed or re-equilibrated during M_3 in the Augusta area in no way affects the conditions of metamorphism deduced for the region. This matter will be considered in detail in a future contribution.